Different roles of dFOXO and HSF in spatio-temporal dynamics of stress-inducible Hsp70 in lgl-yorkie & lgl-Ras driven epithelial tumours in *Drosophila*

Gunjan Singh* and Subhash C. Lakhotia

[1]Cytogenetics Laboratory, Department of Zoology, Banaras Hindu University, Varanasi, 221005, India

*Corresponding author

Email:

Gunjan Singh: gunjan.genetics@gmail.com

S.C. Lakhotia: lakhotia@bhu.ac.in

ORCID ID:

Gunjan Singh: 0000-0002-4458-180X

S.C. Lakhotia: 0000-0003-1842-8411

Running Title: Hsp70 in *Drosophila* tumours

Key words: Neoplastic transformation; Hypoxia; Polarity genes, Tracheoneogenesis; JNK

Abstract

Oncogenic cells recruit diverse cellular survival machineries, including the highly conserved heat shock proteins (Hsps), to counter stressful conditions during tumour progression. Despite important roles of Hsps in several cancers, poor understanding of their regulation leaves major gaps in identifying mechanisms of cellular stress responses exploited by cancer cells. Following our earlier report of stress inducible Hsp70 expression only in a few cells in polarity defective tumorous clones, we now show that Hsp70 is expressed only in neoplastic tumours. Hsp70's expression at 72h after clone induction is mostly limited to a few *lgl*$^{-}$ *yki*^{OE} cells exhibiting mesenchymal features in hypoxic zone closer to tracheae, although all tumorous cells express *hsp70* transcripts. Down-regulation of the *hsp70a* but not *hsp70b* cluster transcripts substantially suppresses growth of *lgl*$^{-}$ *yki*^{OE} clones without affecting their early establishment. However, over-expression of Hsp70 or Hsp70-cochaperone DnaJ suppress *lgl*$^{-}$ *yki*^{OE} clones' growth at early stage. This spatially and temporally regulated expression of Hsp70 in *lgl*$^{-}$ *yki*^{OE} clones is independent of HSF but requires dFOXO and JNK signalling, while a nearly similar pattern of Hsp70 expression in *lgl*$^{-}$ *Ras*^{V12} clones requires HSF, rather than dFOXO. Such context dependent Hsp70 regulation provides novel insight into stress regulatory machinery in cancer cells.

Key words: Apoptosis; Tracheoneogenesis; Hypoxia; Ras; HSF; JNK

Introduction

The endurance of tumour cells to harsher growth conditions and their capacity to escape from drug-induced apoptosis by developing resistance to chemotherapy remain the major challenges in curing cancer (Vasan et al., 2019). Tumour biology research over the past decades has provided significant insights into molecular events associated with oncogenesis, and have shown that resistance to anti-cancer drugs often relies on the cell-stress response pathways, including the regulated expression of the ancient and evolutionarily conserved heat shock proteins (Hsps)(Lang et al., 2019; Zorzi and Bonvini, 2011). Among the cell stress inducible genes, the 70-kDa heat shock protein (Hsp70) is the most conserved and maximally inducible stress protein (Arya et al., 2007; Bukau et al., 2000; Feige and Polla, 1994; Morimoto, 1998; Radons, 2016). It is also known to be overexpressed in human cancers of diverse origins to promote growth, survival and metastasis of cancerous tissue and to be involved in development of drug resistance and suppression of their apoptosis (Juhasz et al., 2013; Leu et al., 2011; Stankiewicz et al., 2005)**.** Hsp70 family of molecular chaperones includes constitutively expressed *hsc70* and stress-inducible *hsp70* genes (Chang et al., 2008; Daugaard et al., 2007; Flaherty et al., 1990; Murphy, 2013). The heat shock factor (HSF1 in human and HSF in *Drosophila*) has been identified as the primary transcription factor regulating stress-induced expression of the diverse heat shock genes, including the Hsp70 (Arya et al., 2007; Cyran and Zhitkovich, 2022; Zorzi and Bonvini, 2011).

In our earlier study (Singh et al., 2022) we found that all the constitutively expressed Hsps like Hsp83, Hsc70, Hsp60 and sHsps were expressed at higher levels since initial stages of epithelial tumours resulting from the loss of cell polarity Lgl protein (lgl^{-}). However, in contrast to the reported over-expression of the stress-inducible Hsp70 in mammalian cancers (Lang et al., 2019), we found that the stress-inducible Hsp70 is expressed only in a few cells of the lgl^{-} yki^{OE} (Yorkie over-expressing) clones at a late stage when the clones appeared to be getting transformed. Unlike in most mammalian cancers, where HSF is known to be essential for oncogenesis (Cyran and Zhitkovich, 2022), we (Singh et al., 2022) found that down- or up-regulation of HSF did not affect growth and transformation of the lgl^{-} yki^{OE} clones.

In the present study we further examined spatio-temporal patterns of expression of the stress-inducible Hsp70 in *Drosophila* larval loss of cell polarity Lgl protein (lgl^{-}) epithelial tumours in different tumour promoting genetic backgrounds and found that the stress-inducible Hsp70

was detectable only in tumours that can become neoplastic. The first appearance of Hsp70 coincided with expression of MMP1 and Ena and accumulation of F-actin in the tumorous clones and was generally limited to a few cells that were closer to tracheae and expressed hypoxia markers like Sima, Tango, Gasp or lactate dehydrogenase (LDH). Interestingly, unlike the limited expression of Hsp70 in the tumorous clones, the *hsp70* transcripts were seen in the all cells in *lgl*$^{-}$ *yki*^{OE} clones at 72 h after clone induction (ACI). Down- regulation of the *hsp70a* cluster transcripts, but not of the *hsp70b* cluster, substantially suppressed transformation of *lgl*$^{-}$ *yki*^{OE} clones without affecting their early establishment; interestingly up-regulation of either of the two *hsp70* gene clusters suppressed early as well as the late-stage *lgl*$^{-}$ *yki*^{OE} clones. We also show that the spatially and temporally regulated expression of Hsp70 in *lgl*$^{-}$ *yki*^{OE} clones is independent of HSF but requires dFOXO and JNK signalling. Significantly, a nearly similar spatial and temporal expression pattern of the stress inducible Hsp70 in *lgl*$^{-}$ *Ras*^{V12} clones requires HSF since down- or up-regulation of HSF suppressed or enhanced, respectively, growth of *lgl*$^{-}$ *Ras*^{V12} clones, but down-regulation of dFOXO caused only a marginal reduction in Hsp70 but did not affect the aggressive growth of *lgl*$^{-}$ *Ras*^{V12} clones. Our finding that regulation and expression of Hsp70 in cancerous cells is highly context dependent has implications for therapeutic approaches that target Hsp70.

Results

Distinct spatio-temporal pattern of stress-inducible Hsp70 in neoplastic epithelial tumours

We have reported earlier (Singh et al., 2022) that while levels of the developmentally expressed Hsps, like Hsp83, Hsc70, Hsp60 and sHsp-Hsp27 is elevated in *lgl*$^{-}$ *yki*^{OE} and *lgl*$^{-}$ *Ras*^{v12} MARCM clonal cells since their early stages, the stress-inducible Hsp70 is expressed only in a sub-set of tumour cells at late stages of the tumour progression. Here we focused on examining the expression of Hsp70 during progression of the tumorous clones. As noted earlier (Singh et al., 2022), only 1 or 2 cells showed Hsp70 staining in only ~3% of the *lgl*$^{-}$ *yki*^{OE} clones (N=105) at 48hr ACI. With increased tumor age, the frequency of Hsp70-positive clones increased to 10% (N= 68 clones), 18% (N= 82 clones) and 46% (N=44 clones) at 51hr, 54hr and 72hr ACI, respectively. As also noted earlier (Singh et al., 2022), at 72hr ACI, the Hsp70 expressing clones became more frequent. Interestingly, however, in a majority of the 132 clones examined from 68 discs a strong expression of Hsp70 was limited to only a few cells with little staining for Hsp70 in rest of the clone area (Fig. 1A-A'). In a few clones (72hr ACI),

the entire clone area also showed Hsp70 at a low level with some cells showing a much higher Hsp70 staining (see Fig. 3d-e in (Singh et al., 2022)) . With advancing clone age, increasing numbers of *lgl*$^{-}$ *yki*^{OE} tumorous clones and cells within them were found to express Hsp70 so that by 144hr ACI, the entire disc appeared Hsp70 positive with patches of stronger expression (Fig. 1B-D').

We next examined expression of Hsp70 in *lgl*$^{-}$ *Ras*^{v12} clones, which express the other Hsps as in the *lgl*$^{-}$ *yki*^{OE} clones (Singh et al., 2022). The Hsp70 expression in these tumorous clones (Fig. 1E-G') also followed a pattern generally similar to that noted above for *lgl*$^{-}$ *yki*^{OE} clones except that the frequency of Hsp70 positive *lgl*$^{-}$ *Ras*^{v12} clones at 72hr ACI was somewhat lower than in same age discs carrying *lgl*$^{-}$ *yki*^{OE} clones (Fig. 1E, E'), and Hsp70, when present, was usually seen at a lower level across the entire *lgl*$^{-}$ *Ras*^{v12} clone with a few cells having higher levels (Fig. 1E-G'). However, this difference between *lgl*$^{-}$ *yki*^{OE} and *lgl*$^{-}$ *Ras*^{v12} tumorous clones became less apparent as the tumorous clones advanced in their size and malignancy with age.

An analysis of transformation of *lgl*$^{-}$ *yki*^{OE} clones, indicated by nucleation and accumulation of F-actin, and presence or absence of some Hsp70 positive cells in them indicated that Hsp70 positive cells were more frequently seen in clones with high F-actin accumulation, an indication of their transformation. In order to analyze this, we examined relation between clone size, F-actin accumulation and Hsp70 expression in different clones at 72hr ACI. We selected discrete GFP^{+} *lgl*$^{-}$ *yki*^{OE} clones that were larger than 1µm^2 area (but smaller than 6µm^2 area, to avoid fused clones); they were considered F-actin^{+} or Hsp70^{+} only if the F-actin and Hsp fluorescence signal intensity in the clone were >0.02/pixel and >0.005/pixel, respectively. These threshold fluorescence intensities were greater than the background, which was estimated in randomly selected non-clonal GFP^{-} areas in the discs carrying the analyzed clone/s (N = 53 clones). Accordingly, each clone was classified as F-actin^{+} or F-actin^{-} and Hsp70^{+} or Hsp70^{-}. As the Venn diagram in Fig. 1I shows, nearly 40% clones showed high levels of F-actin as well as Hsp70. It may be noted that some high F-actin enriched clones may have been classified as low Hsp70 because only a few cells in them were Hsp70+ve and thus on the per pixel basis, they may get classified as Hsp70-low.

We also noticed that the Hsp70 positive cells in transformed clones often showed mesenchymal appearance with cytoplasmic extensions/protrusions (Fig. 1C, D, also see later).

The F-actin rich *lgl*$^{-}$ *yki*^{OE} clones in other larval tissues like eye-antennal discs (Fig. 1J, J') or brain ganglia (Fig. 1K, K') also showed only a few of the clonal cells to be positive for Hsp70 expression at 72hr ACI. These results suggest that the expression of Hsp70 in a few *lgl*$^{-}$ *yki*^{OE} clonal cells at 72hr ACI is a common feature and is in some way related to the beginning of transformation of the clones.

Expression of the stress inducible Hsp70 in tumors of different genetic backgrounds correlates with their transformation potential

Presence of only a few Hsp70^{+} cells in a sub-set of the late stage of tumour clones, indicate specific regulatory events that restrict this protein's induction only in a few cells. Therefore, we also examined Hsp70 expression in non-neoplastic and neoplastic tumors of different genetic backgrounds. Non-neoplastic *lgl*$^{-}$ MARCM clones (Fig. 2A), or tissues with loss of polarity as in *MS1096>lgl*^{RNAi} (Fig. 2B) did not express Hsp70 in any cell even at later larval stages. On the other hand, single hit malignant tumors like *Act>lgl*^{RNAi} (Fig. 2C-D) or *MS1096>yki*^{Act} (Fig. 2E-F) or *MS1096>Pvr*^{Act} (Fig. 2G-H) as well as multiple hit malignant tumors like *MS1096>Ras*^{V12} *lgl*^{RNAi} (Fig. 2I-J) or *MS1096>Ras*^{V12} *Scrib*^{RNAi} (Fig. 2K-L) showed Hsp70 expression, initially in a limited cells/area of the growing tumor which spread to near uniformity throughout older tumorous clones/area in older larvae (Fig. 2C-L). It is notable that while non-neoplastic *lgl*$^{-}$ clones or hyperplastic *MS1096>lgl*^{RNAi} wing discs with *lgl* down regulated only in wing discs (Fig. 2A-B) did not show Hsp70 expression, loss of cell polarity in the entire organism (*Act>lgl*^{RNAi}), which is known to cause neoplasia (Bunker et al., 2015; Li et al., 2020), induced Hsp70 in tumorous discs (Fig. 2C-D). These results (summarized in Table 1) indicate that Hsp70 expression and neoplastic transformation in epithelial tumours of different genetic backgrounds are associated events.

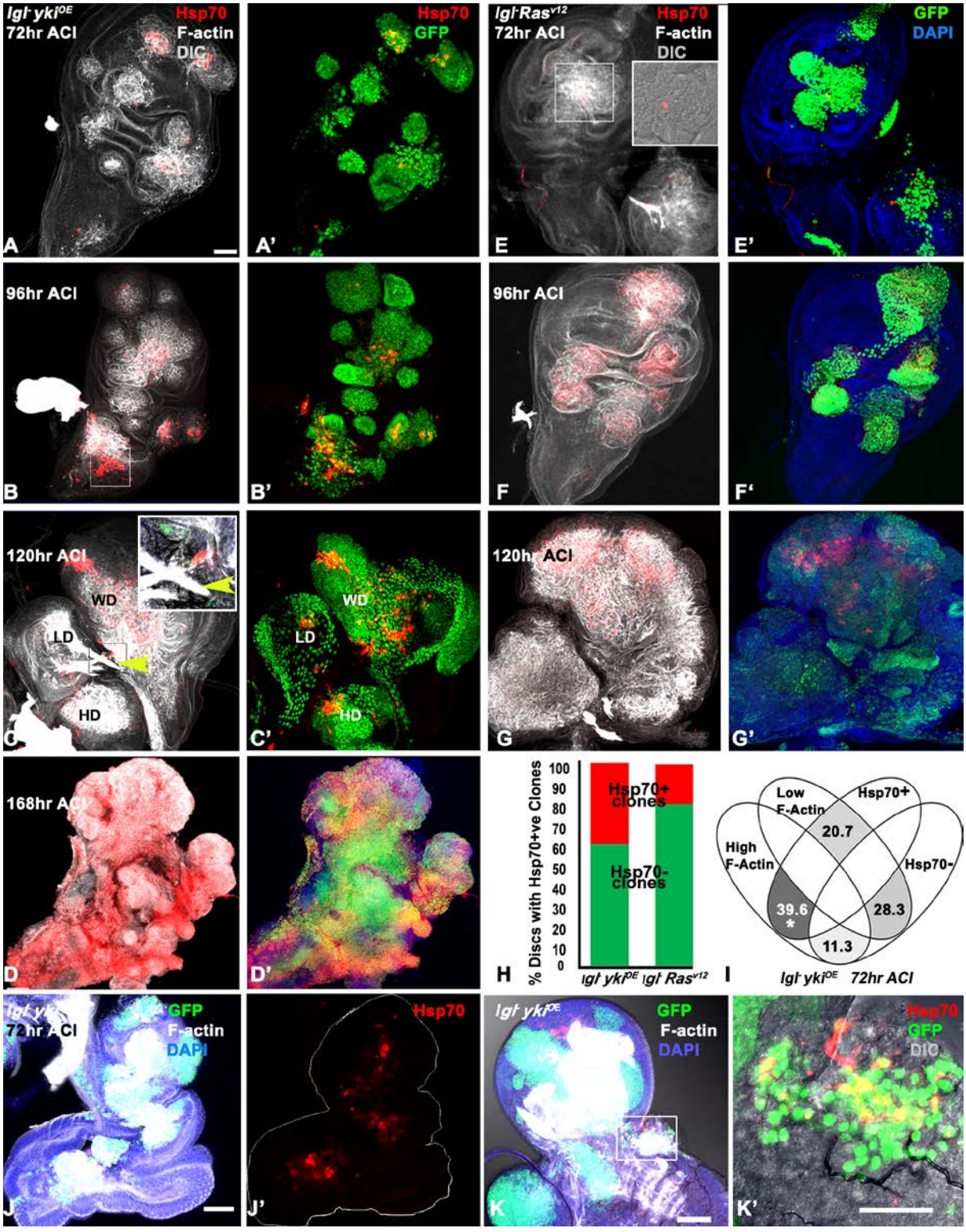

Fig. 1. Expression of stress-inducible Hsp70 is spatio-temporally regulated in *lgl- yki^{OE}* and *lgl- Ras^{v12}* clones. A-D': Confocal projection images of wing imaginal discs carrying *lgl- yki^{OE}* clones at different hours ACI (noted on upper left corner in each case) showing distribution of Hsp70 (red), GFP (green), F-actin (white); inset in **C** is a magnified view of the boxed area to show mesenchyme cell like appearance of some of the Hsp70^{+} clonal cells; **HD, LD** and **WD** in **C-C'** are partially fused haltere, leg and wing imaginal discs, respectively; yellow arrow heads in **C-C'** point to F-actin cable traversing LD and WD along with an

associated Hsp70^{+} clonal cell. **E-G':** Confocal projection images of wing imaginal discs carrying *lgl^{-} Ras^{v12}* clones at different hours ACI (noted on upper corner in each case) showing distribution of Hsp70 (red) in GFP positive (green) clones, F-actin (white in **E-G**) and DAPI (for chromatin, blue in **E'-G'**); inset in **E** shows Hsp70 staining against DIC image of the F-actin rich boxed area. **H:** Stacked bar diagrams to show relative frequencies (Y-axis) of *lgl^{-} yki^{OE}* (138 clones from 48 wing discs) and *lgl^{-} Ras^{v12}* (105 clones from 36 discs) clones (X-axis) with (red) or without (green) Hsp70^{+} cells at 72hr ACI. **I:** Venn diagram showing coincidence of *lgl^{-} yki^{OE}* clones with high F-Actin aggregates and presence of Hsp70+ cells at 72hr ACI (total clones examined = 112). **J-K'**: Confocal projection images of eye-antennal disc (**J, J'**) and brain ganglia (**K, K'**) carrying *lgl^{-} yki^{OE}* clones at 72hr ACI showing Hsp70 (red in **J', K** and **K'**), F-actin (white in **J** and **K**) and DAPI (blue in **J** and **K**); **J'** shows only Hsp70 in the eye-antennal disc (outlined with white line) shown in **J,** while **K'** is an enlarged image of the brain region boxed in **K** showing Hsp70 (red), GFP (green) and DIC (grey). Scale bar in **A** = 50µm and applies to **A'-G'**, in **J** = 50µm, applies also to **J'**, in **K** = 50µm and that in **K'** = 20µm.

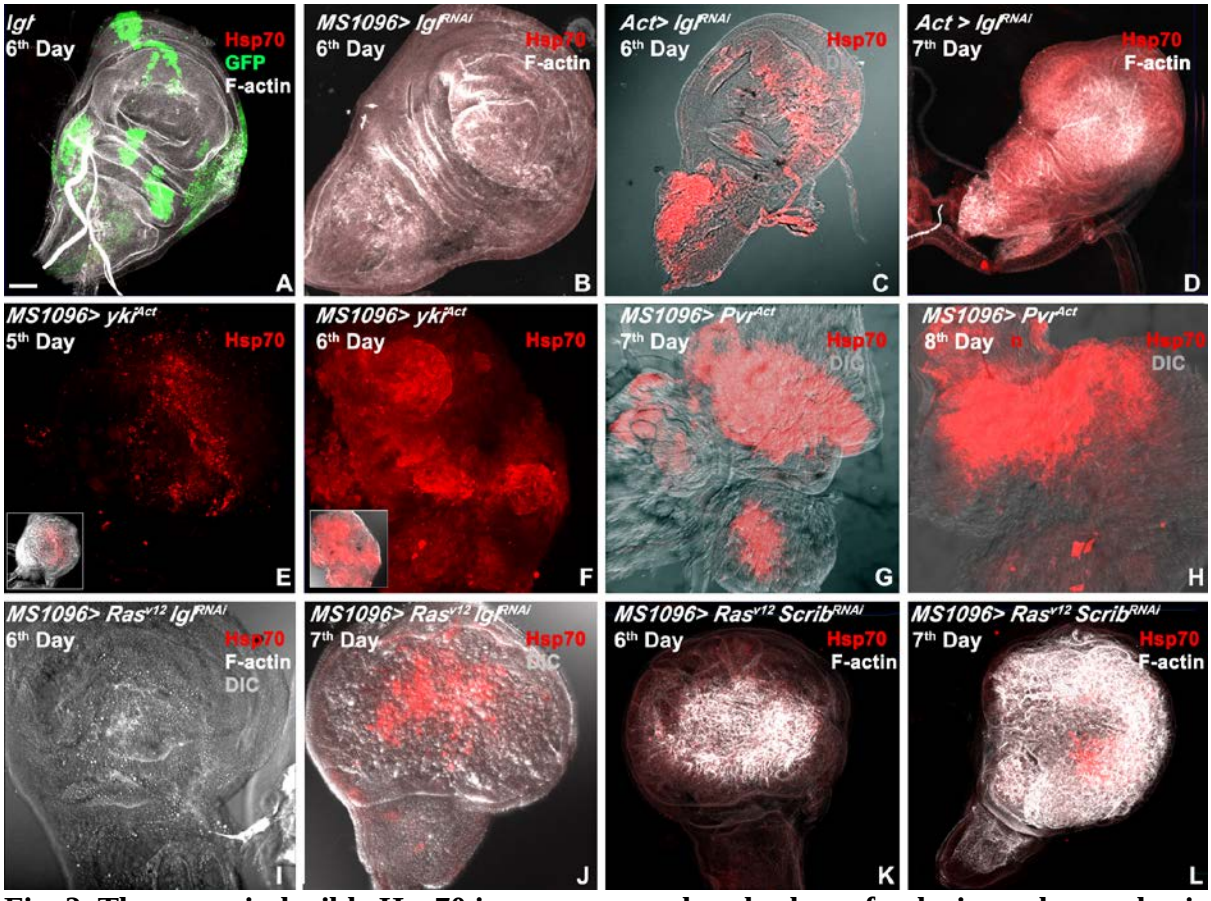

Fig. 2. The stress inducible Hsp70 is not expressed under loss of polarity or hyperplastic condition but is expressed only in tumours that get transformed. A-L: Confocal projection images of wing discs (genotypes noted on the top left corner in each case) showing Hsp70 (red) and F-actin (white), DIC (gray); panel in **A** also shows GFP (green) in the *lgl^{-}* MARCM clones at 96hr ACI; larval age in is indicated on upper left corner of each panel as days after egg laying. Insets in **E** and **F** show low magnification images, including the DIC and Hsp70 staining, of the respective wing discs. Scale bar in A represents 50µm and applies to A-L.

Table 1. The stress inducible Hsp70 protein is expressed only in loss of polarity associated epithelial tumours which have potential to become malignant

Genotype of tumorous tissue	**Nature of the mutation**	**Nature of Tumour**	**Hsp70 expression**	**Figure**
lgl^{-} MARCM clones	Loss of polarity in clones	Non-malignant hyperplastic	No	Fig. 2A
MS1096> lgl^{RNAi}	Loss of polarity in wing blade	Non-malignant hyperplastic	No	Fig. 2B
MS1096>Scrib^{RNAi}	Loss of polarity in wing blade	Non-malignant hyperplastic	No	Not shown
Act> lgl^{RNAi}	Loss of polarity in all cell types	Malignant	Yes	Fig. 2C-D
MS1096>Yki^{Act}	Active Yorkie over-expression in wing blade	Malignant	Yes	Fig. 2E-F
MS1096>Pvr^{Act}	Over-expression of Ras/Raf/MAP kinase (ERK) cascade activator in wing blade	Malignant	Yes	Fig. 2G-H
MS1096>lgl^{RNAi}*Ras*^{V12}	Loss of cell polarity and expression of Activated Ras in wing blade	Malignant	Yes	Fig. 2I-J
MS1096>Scrib^{RNAi}*Ras*^{V12}	Loss of cell polarity and expression of Activated Ras in wing blade	Malignant	Yes	Fig. 2K-L
lgl^{-} *Yki*^{OE} MARCM clones	Loss of cell polarity with Yorkie over-expression	Malignant	Yes	Fig. 1A-D’
lgl^{-} *Ras*^{V12} MARCM clones	Loss of cell polarity with activated Ras over-expression	Malignant	Yes	Fig. 1E-G’

Unlike Hsp70 protein, the *hsp70* transcripts are present in all cells of *lgl^{-} yki^{OE}* clones

In order to see if the limited expression of the stress-inducible Hsp70 in *lgl^{-} yki^{OE}* clones correlated with transcriptional activation of the *hsp70* genes in those cells, we carried out in situ hybridization to cellular RNA in wing imaginal discs carrying *lgl^{-} yki^{OE}* clones at 72hr ACI using a Cy3-tagged oligonucleotide probe that can hybridize to the stress inducible *hsp70* transcripts from all the multiple gene copies present in *D. melanogaster*. *Drosophila melanogaster* carries two clusters of the stress inducible *hsp70* genes at the 87A and 87C cytogenetic regions of right arm of chromosome 3, with the former cluster having 2 copies (*hsp70A* group) and the later 3-4 copies (*hsp70B* group) of *hsp70* genes all of which carry nearly identical coding sequences (Ish-Horowicz et al., 1979). Surprisingly, unlike the limited expression of the Hsp70 protein, the *hsp70* transcripts were present in nearly all the clonal cells at 72hr ACI (Fig. 3A-B). Co-immunostaining with the Hsp70 antibody and RNA in situ hybridization in these discs (Fig. 3B) confirmed that only a small number of all the *hsp70* transcript positive clonal cells show presence of Hsp70. The *hsp70* transcripts were present in cytoplasm as well nuclei of these cells. Interestingly, the nuclear transcripts were mostly seen as two adjacent bright spots (Fig. 3A", B), which seem to represent the sites of transcription of the *hsp70* gene copies. At first sight it may appear that the two bright hybridization signals seen in the *lgl^{-} yki^{OE}* clonal cell nuclei (Fig. 2A", B) may represent the two gene clusters on synapsed homologs. However, this appears unlikely since the small size of the imaginal disc nuclei would not permit resolution of the two closely located gene clusters, unlike in the large polytene chromosomes. Instead, it is likely that the two adjacent bright hybridization signals in each nucleus represent transcriptionally active *hsp70* genes on the two homologs.

These results suggest that the synthesis of Hsp70 protein in a limited set of cells in the *lgl^{-} yki^{OE}* clones is a consequence of post-transcriptional regulation.

Down-regulation of transcripts of the *hsp70A*, but not *hsp70B* group, or up-regulation of *hsp70* transcripts suppresses growth of lgl^{-} yki^{OE} clones

It is known from earlier studies that the *hsp70* genes present at the two clusters can show differential transcriptional induction in different tissues following heat shock (Lakhotia and Prasanth, 2002). Therefore, to know if genes at both the *hsp70* gene clusters or the gene copies from one of them only become transcriptionally active in *lgl^{-} yki^{OE}* clonal cells, we down-regulated *hsp70* transcripts from the *hsp70A* or the *hsp70B* cluster or over-expressed the

hsp70A coding region in *lgl^{-} yki^{OE}* clones by co-expressing specific transgenes and monitored growth of the tumorous clones in each case and survival of larvae of the different genetic backgrounds to adult hood (Fig. 3C-N).

Down-regulation of *hsp70A* gene cluster transcripts by co-expression of *Hsp70A^{RNAi}* transgene did not significantly affect (P>0.05 on Mann-Whitney test) the numbers of *lgl^{-} yki^{OE} Hsp70A^{RNAi}* GFP-positive clones/disc at 48hr ACI (N=46 wing discs) when compared with similar age *lgl^{-} yki^{OE}* controls (N=57 wing discs, Figs. 3C, D). Interestingly, however, over expression of *hsp70A* transcripts in *lgl^{-} yki^{OE} Hsp70A^{OE}* clones also resulted in very few clones (N=47 discs) at 48hr ACI (Fig. 3E). When examined at 72hr ACI, the *lgl^{-} yki^{OE} Hsp70A^{RNAi}* or *lgl^{-} yki^{OE} Hsp70A^{OE}* clones per disc were fewer than *lgl^{-} yki^{OE}* clones (Fig. 3 F-H'). In order to assess the rate of growth of individual clones of these genotypes, we compared the % clonal area (cumulative area of all clones in the pouch region expressed as % of the total area of pouch region in the disc, see (Singh et al., 2022)) occupied by *lgl^{-} yki^{OE} Hsp70A^{RNAi}* or *lgl^{-} yki^{OE} Hsp70A^{OE}* clones in wing discs with the % clonal area of the *lgl^{-} yki^{OE}* clones at 48hr (Fig. 3I) and 72hr (Fig. 3J) ACI. While the % clonal areas of *lgl^{-} yki^{OE}* and *lgl^{-} yki^{OE} Hsp70A^{RNAi}* clones at 48hr ACI were not significantly different (Fig. 3I), that of *lgl^{-} yki^{OE} Hsp70A^{OE}* clones was significantly less than of the *lgl^{-} yki^{OE}* clones at this time point. On the other hand, at 72hr ACI, the % clonal areas occupied by *lgl^{-} yki^{OE} Hsp70A^{RNAi}* or the *lgl^{-} yki^{OE} Hsp70A^{OE}* clones were significantly less than of the *lgl^{-} yki^{OE}* clones of same age (Fig. 3J).

We then examined if the poorer growth of *lgl^{-} yki^{OE} Hsp70A^{RNAi}* or *lgl^{-} yki^{OE} Hsp70A^{OE}* clones at 72hr ACI, as reflected in their reduced % clonal areas, was associated with enhanced apoptosis by immunostaining wing discs at 72hr ACI carrying *lgl^{-} yki^{OE}* or *lgl^{-}yki^{OE} Hsp70A^{RNAi}* or *lgl^{-} yki^{OE} Hsp70A^{OE}* clones for Dcp-1, the executive apoptotic caspase (Tamori et al., 2016). As shown in Fig. 3F-H', *lgl^{-} yki^{OE}* tumorous clones with down- or up-regulated Hsp70 showed higher levels of Dcp-1 staining than the same age *lgl^{-} yki^{OE}* clones. A qualitative assessment of clones with apparent high or low/negligible Dcp-1 staining in clones of these three genotypes at 72hr ACI (Fig. 3K) confirmed that frequencies of clones with higher levels of active Caspase-3 were greater when *Hsp70A^{RNAi}* or *Hsp70A^{OE}* transgene was co-expressed in *lgl^{-} yki^{OE}* clones.

We next assayed if the above effects on altered growth of the *lgl^{-} yki^{OE}* clones when the *hsp70A* genes are down-or up-regulated, have organism level consequences. For this, we compared the survival of the host larvae carrying clones of different genotypes to pupal and adult stages. As shown in Fig. 3N, compared to larvae (N=426) carrying *lgl^{-} yki^{OE}* clones, fewer of those carrying

lgl^{-}*yki*^{OE} *Hsp70A*^{RNAi} (N=460) or *lgl*$^{-}$ *yki*^{OE} *Hsp70A*^{OE} (N=340) clones died as psuedopupae but continued to develop so that more of them emerged as adults.

We also examined if co-expression of *Hsp70B*^{RNAi} in *lgl*$^{-}$ *yki*^{OE} clones affected host-survival. Interestingly, these larvae (N=410) formed pseudopupae as frequently as larvae carrying *lgl*$^{-}$ *yki*^{OE} clones, resulting in fewer adult survivors (Fig. 3N). It appears, therefore, that directed down-regulation of *hsp70B* cluster of genes by co-expressing the *Hsp70B*^{RNAi} does not affect growth of *lgl*$^{-}$ *yki*^{OE} clones, suggesting that the *hsp70B* cluster genes are not active in these tumorous clones.

We also examined if up-regulation of DnaJ, a cochaperone of Hsp70 (Arya et al., 2007), affected growth of *lgl*$^{-}$*yki*^{OE} clones. Similar, to the effect of Hsp70 over-expression on the tumour growth, over-expression of DnaJ in these clones also reduced their numbers at 48hr as well as 72hr ACI (Fig. 3L, M) with high Dcp-1 activity in the surviving clones (Fig. 3M').

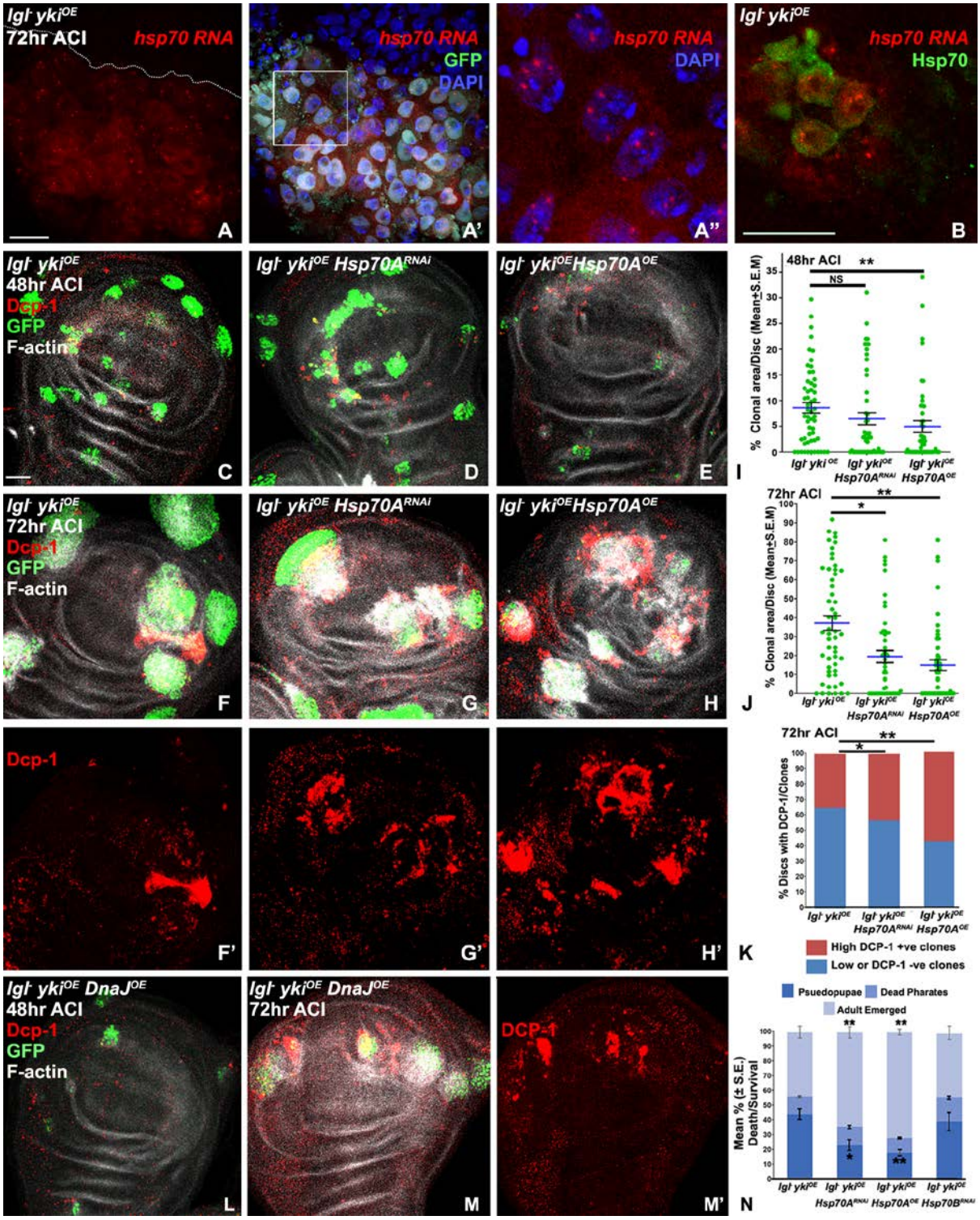

Fig. 3. Unlike Hsp70 protein, *hsp70* transcripts are present in all *lgl⁻ yki^{OE}* clonal cells and targeted down- or up-regulation of *hsp70A* cluster of genes in *lgl⁻ yki^{OE}* clones results in their poorer growth and, therefore, better survival of host larvae. A-B: Confocal images (projection in **A-A'**, optical sections in **A"** and **B**) showing distribution of the stress-inducible *hsp70* RNA (red) and Hsp70 protein (green in **B**) in wing discs carrying *lgl⁻ yki^{OE}* clones at 72hr ACI; dotted line in **A** indicates the border of the GFP+ clone (green in **A'**); the boxed area in **A'** is shown at higher magnification in **A"**; DAPI (blue) fluorescence is also shown in **A'-A"**. **C-H'**: Confocal projection images of wing discs carrying *lgl⁻ yki^{OE}* (**C, F-F'**), *lgl⁻ yki^{OE}*

Hsp70A^{RNAi} (**D, G-G'**), *lgl*$^{-}$ *yki*^{OE} *Hsc70A*^{RNAi} (**E, H-H'**) clones showing Dcp-1 (red) and F-actin (white) in GFP expressing (green) clones at 48hr (**C-E**) or at 72hr (**F-H'**) ACI. **I-J:** Scatter plots showing % Clonal area/Disc (Mean±S.E., Y-axis) at 48hr (**I**) and 72hr ACI (**J**) in different genotypes (X axis). **K**: Bar graph histograms show % of wing discs (Y-axis) with GFP positive clones of different genotypes (X-axis) expressing Dcp-1 at negligible/low (blue shaded region) or high (red shaded region) levels at 72hr ACI. **L-M'**: Confocal projection images of wing discs carrying *lgl*$^{-}$ *yki*^{OE} *DnaJ*^{OE} clones showing Dcp-1 (red) and F-actin (white) in GFP expressing (green) clones at 48hr (**L**) or at 72hr (**M-M'**); **M'** shows only the Dcp-1 staining in the disc in **M**. ACI. **N**: Bar histograms showing Mean % (± S.E.) death (as pseudopupae or pharate) and survival as adults (Y-axis) of the 72hr old larvae exposed to a 3min HS at 72hr AEL to induce *lgl*$^{-}$ *yki*^{OE} somatic clones in different genetic backgrounds (*lgl*$^{-}$ *yki*^{OE}, *lgl*$^{-}$ *yki*^{OE} *Hsp70A*^{RNAi}, *lgl*$^{-}$ *yki*^{OE} *Hsp70A*^{OE}, and *lgl*$^{-}$ *yki*^{OE} *Hsp70B*^{RNAi}, X-axis). In all the scatter plot/bar graphs, the thick horizontal blue bar indicates the mean while a vertical black bar indicates the ±S.E.M.; the thick horizontal black lines in **O** and **P** on top indicate the pairs of scatter plots tested for statistical significance; in **R**, comparisons were made with the respective values of death/survival of *lgl*$^{-}$ *yki*^{OE} clone carrying larvae; the p-values are indicated as: n.s. = >0.05, * =<0.05 and ** =<0.01. Scale bar in A = 50µm and applies to A'-A'', in B = 50µm, in C = 50µm and applies to C-H' and L-M'.

Cells expressing high levels of Hsp70 at 72hr ACI in *lgl*$^{-}$ *yki*^{OE} clones show mesenchymal markers, are often close to tracheae, and express hypoxia markers

As noted earlier (Fig. 1), the Hsp70 expressing *lgl*$^{-}$ *yki*^{OE} clonal cells often showed extensions like those seen in mesenchymal cells (Fig. 4A). In agreement, the Hsp70 expressing clonal cells specifically showed mesenchymal markers like MMP1 and Ena (Gates et al., 2007; Lodge et al., 2021; Sano et al., 2012) at high levels (Fig. 4B-C), which further suggested their transition to mesenchymal fate. Further, in a few instances such cells could be seen to be moving out of the imaginal disc into a neighbouring tissue (Fig. 4C').

Unlike vertebrates, insects like *Drosophila* have an open circulatory system and use branched and interconnected fine tracheal tubules to directly facilitate gaseous exchange between cells in different organs and the atmosphere (Medioni et al., 2009). Like the vascularization of vertebrate cancers, tracheal tubes are recruited to oxygenate the growing tumorous mass in *Drosophila* (Calleja et al., 2016; Grifoni et al., 2015; Mirzoyan et al., 2019). We examined if the few Hsp70 expressing cells had any anatomical co-ordinates in relation to the tracheal system in the tumorous clones. Interestingly, the Hsp70^{+} cells were found to be mostly present in proximity of tracheae in *lgl*$^{-}$ *yki*^{OE} clones in wing as well as eye discs at 72hr ACI (Figs. 4D-F, Fig. S1) where high F-actin accumulation was also seen.

In view of close proximity of tracheae and Hsp70^{+} cells in tumorous clones, we examined co-localization of hypoxia markers like Sima (fly homolog of HIF-α transcription factor mediating

hypoxic response), Lactic dehydrogenase (LDH), or tracheal markers like Gasp and Tango (Sonnenfeld et al., 1997; Tsarouhas et al., 2007) and Hsp70 in wing imaginal discs carrying *lgl*$^{-}$ *yki*^{OE} clones at 72hr ACI. The LDH was detected by expressing hypoxia-sensitive reporter transgene *LDH-LacZ*, which produces β-galactosidase under the *LDH* promoter (Sansone and Blumenthal, 2013).

High level of Sima staining was seen in the clonal areas around tracheae where Hsp70^{+} cells were also clustered (Fig. 4G-G'). Immunostaining for the *LacZ* encoded β-galactosidase in *lgl*$^{-}$ *yki*^{OE} clones co-expressing the hypoxia-sensitive reporter *LDH-LacZ* transgene showed high *LDH-LacZ* expression in Hsp70^{+} cells and the surrounding area (Fig. 4H-H'). At 72hr ACI, many Hsp70^{+} cells, located near tracheal branches, also co-expressed the tracheal markers Gasp (Fig. 4I-I') and Tango (Fig. 4J-J').

Since expression of HIF-α, mammalian homolog of *Drosophila* Sima, is known to regulate *hsp70* transcription (Sarge et al., 1993, Wu 1995; Baird et al., 2006, Tsuchida et al., 2014, Masser et al., 2020), we examined if over-expression of Sima in the pouch region of otherwise normal wing discs affects Hsp70 expression by immunostaining for Hsp70 in *MS1096>Sima*^{OE} larvae. These discs showed slightly defective morphology and showed a low expression of Hsp70 in some cells in the pouch region (Fig. 4K). When *lgl*^{RNAi} was co-expressed in these discs (*MS1096>Sima*^{OE} *lgl*^{RNAi}), the pouch region appeared slightly hyperplastic, and more cells showed Hsp70 expression (Fig. 4L) than in *MS1096>Sima*^{OE} discs. The wings in *MS1096>Sima*^{OE} (Fig. K') were small with necrotic marks in the distal region; interestingly the wings in *MS1096>Sima*^{OE} *lgl*^{RNAi} flies were more damaged with most of the wing tissue appearing to have suffered necrosis (Fig. 4L').

These results thus suggest a causal relation between tumor induced hypoxia, tracheoneogenesis and expression of Hsp70 in advancing neoplastic clones.

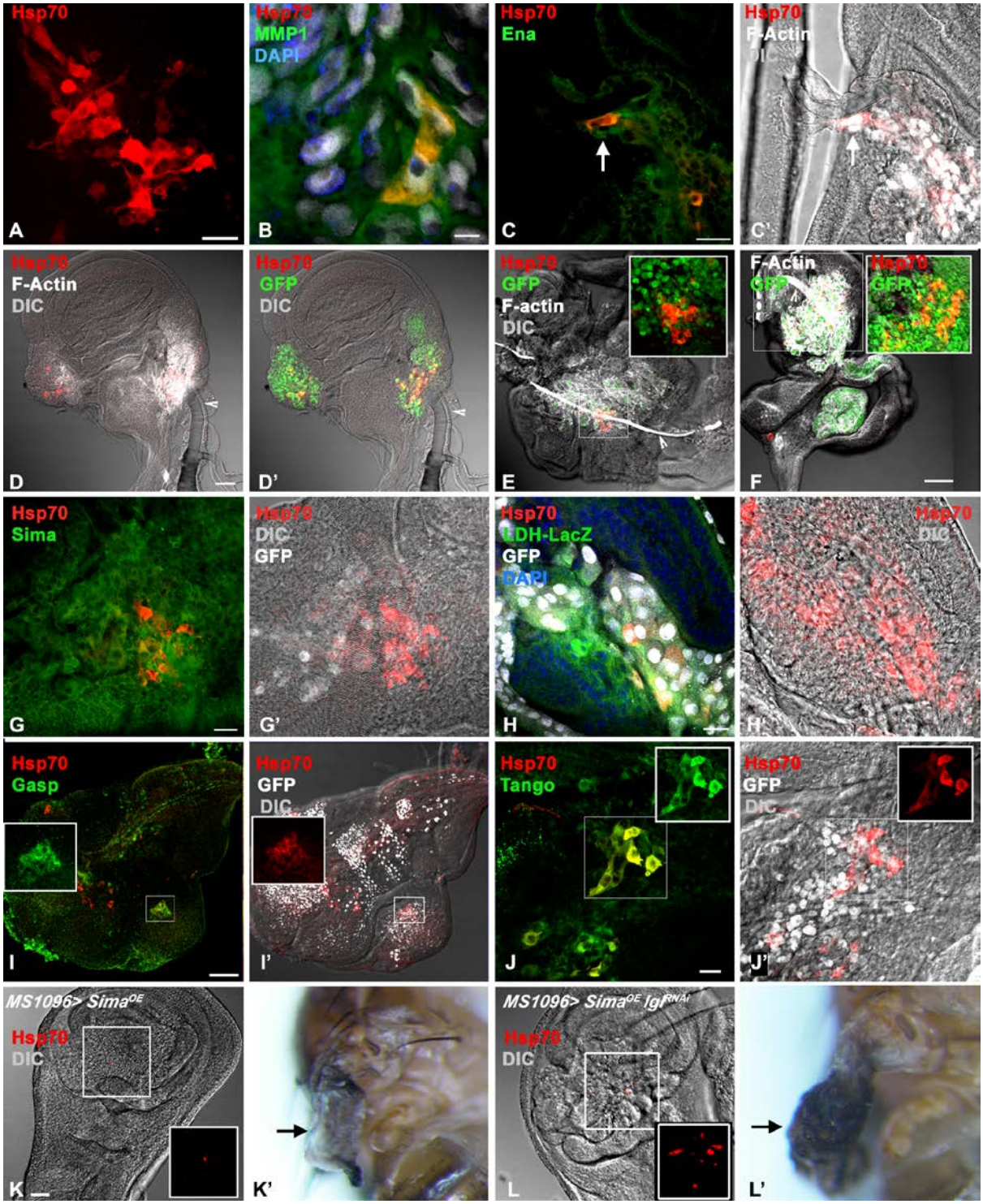

Fig. 4. The Hsp70 expressing cells in *lgl*$^{-}$ *yki*^{OE} clones close to tracheae have mesenchymal appearance with hypoxia marks, and overexpression of Sima leads to Hsp70 expression in some cells of wing discs and damage to wings. A-D': Confocal optical sections of Hsp70+ cells in *lgl*$^{-}$ *yki*^{OE} wing disc clones at 72hr ACI showing Hsp70 (red, **A-D**), MMP1 (green, **B**), Ena (green, **C**), and F-actin (white, **D**) in DIC (grey, **D**) background; **C'** shows combined Hsp70 (red), F-actin (white) and DIC image (Gray) of the disc in **C** while **D'** shows combined Hsp70 (red), GFP (green) and DIC (gravy) image of that in **D**. **E, F:** Confocal optical sections of eye-antennal discs at 72hr ACI showing distribution of Hsp70 (red) and F-actin (white) in GFP positive (green) *lgl*$^{-}$ *yki*^{OE} clones; the insets in **E** and **F** are confocal optical sections of the boxed regions of eye (**E**) and antennal (**F**) discs, respectively; white arrowheads in **D-F'**

indicate tracheae. **G-J'**: Confocal optical sections of wing imaginal discs at 72hr ACI showing distribution of Hsp70 (red) in relation to different hypoxia/tracheal marker proteins (Sima in **G-G'**, LDH-LacZ in **H-H'**, Gasp in **I-I'**, and Tango in **J-J'** in green), in GFP positive (white) *lgl*$^{-}$ *yki*^{OE} clones; DIC (Gray) images are included in **G'-J'**; insets in **I-J'** show only Gasp (Green, **I**) or Hsp70 (red, **I'**, **J'**) or Tango (green, **J**), in the boxed areas in **I-J**, respectively. **K-L** Optical sections showing distribution of Hsp70 expressing cells (red) in *MS1096GAL4>UAS-Sima*^{OE} wing discs without (**K**) or with co-expression of *lgl*^{RNAi} (**L**); DIC image is shown in grey; K'-L' images of wings (indicated by arrows) of *MS1096GAL4>UAS-Sima*^{OE} adult flies without (**K'**) or with co-expression of *lgl*^{RNAi} (**L'**). Scale bar in **A** = 20µm, **B** = 5µm, **C** = 20µm and applies to **C**', in **D** = 50µm and applies to **D'**, in **F** = 50µm and applies to E, in **G** = 20µm and applies to **G'**, in **H** = 20µm and applies to **H'**, in **I** = 50µm and applies to **I**', in **J** = 20µm and applies to **J'**, in **K** = 50µm and applies to **L**.

Expression of Hsp70 in *lgl*$^{-}$ *yki*^{OE} clones is HSF-independent

Expression of Hsp70 and other major Hsps is primarily regulated at the transcription level by the HSF (Masser et al., 2020; Sarge et al., 1993; Wu, 1995). It is also reported that Hsp70 expression in tumours may be linked with activation of HSF by the key hypoxia sensing transcription factor HIF-α/Sima (Baird et al., 2006; Tsuchida et al., 2014). As noted above (Fig. 4), levels of Sima were higher in Hsp70 expressing zone in the *lgl*$^{-}$ *yki*^{OE} clones at 72hr ACI and over-expression of Sima in wing discs also induced Hsp70 to some extent. Therefore, to know if the Hsp70 expression in the *lgl*$^{-}$ *yki*^{OE} clonal cells is HSF dependent, we co-expressed *HSF*^{RNAi} or *HSF*^{OE} transgene to down- or up-regulate, respectively, cellular levels of HSF and assayed Hsp70 in these clones.

We had earlier seen (Singh et al., 2022) that up- or down-regulation of HSF in *lgl*$^{-}$ *yki*^{OE} clones did not affect their growth and transformation. In agreement, we found that despite the near absence or very high levels of HSF in *lgl*$^{-}$ *yki*^{OE} *HSF*^{RNAi} (Fig. 5B) and *lgl*$^{-}$ *yki*^{OE} *HSF*^{OE} (Fig. 5C) clones, respectively, the pattern and level of Hsp70 remained as in the *lgl*$^{-}$ *yki*^{OE} clones (Fig. 5A) at 72hr ACI. Quantification of Hsp70 levels in clones of these three genotypes confirmed that levels of expression of Hsp70 were not affected by HSF levels since the mean Hsp70 intensity per clone in *lgl*$^{-}$ *yki*^{OE} *HSF*^{RNAi} (N=36, clones) and *lgl*$^{-}$ *yki*^{OE} *HSF*^{OE} (N=37, wing discs) remained comparable to that in the *lgl*$^{-}$*yki*^{OE} (N=37, clones) (Fig. 5D).

The spatio-temporally regulated expression of Hsp70 in *lgl*$^{-}$ *yki*^{OE} being independent of the HSF, raised the possibility that other transcription factors may directly or indirectly regulate Hsp70 expression in these clones. Since the dFOXO transcription factor has also been shown to regulate expression of Hsp70 under oxidative stress conditions (Donovan and Marr, 2016), we next examined dFOXO's role in Hsp70 expression in these clones.

dFOXO and JNK pathways regulate the spatio-temporal expression of Hsp70 in *lgl^{-} yki^{OE}* tumors and their neoplastic growth

Co-immunostaining for Hsp70 and dFOXO in *lgl^{-} yki^{OE}* clones at 72hr ACI showed Hsp70 expression only in clones that had higher levels of dFOXO. The example in Fig. 5E shows that of the two *lgl^{-} yki^{OE}* clones in this disc, the larger one (marked 2) with elevated levels of dFOXO shows a few Hsp70^{+} cells while no Hsp70^{+} cell is present in the smaller clone (marked 1) with low dFOXO levels as in the surrounding non-tumorous cells. Interestingly, as shown in Fig 5F-H, the Hsp70 expression was significantly reduced in clones with either down- or up-regulated levels of dFOXO following co-expression of *dFOXO^{RNAi}* (*lgl^{-} yki^{OE} dFOXO^{RNAi}*) or *dFOXO^{OE}* (*lgl $^{-}$yki^{OE} dFOXO^{OE}*) when compared with *lgl^{-} yki^{OE}* control clones. Comparison of intensity of Hsp70 staining in *lgl^{-} yki^{OE}* (N=37 clones) or *lgl^{-} yki^{OE} dFOXO^{RNAi}* (N=36 clones) or *lgl $^{-}$yki^{OE} dFOXO^{OE}* (N=37 clones) clones indeed revealed that lowered as well as enhanced levels of dFOXO significantly reduced Hsp70 levels (Fig. 5I). Comparison of the numbers of clones/disc (Fig. 5J) or the % Clonal area/disc at 72hr ACI (Fig. 5K) revealed that, in agreement with above results, the reduced expression of Hsp70 following down- or up-regulation of dFOXO negatively affected growth of *lgl $^{-}$yki^{OE}* clones.

Since high level of p-JNK is a feature of transformed cells (Muzzopappa et al., 2017; Uhlirova and Bohmann, 2006) and activation of dFOXO involves JNK signalling (Jiramongkol and Lam, 2020; Tafesh-Edwards and Eleftherianos, 2020), we examined expression of JNK in *lgl^{-} yki^{OE}* clones at 72hr ACI. As shown in Fig. 5L, GFP-expressing clones showing presence of Hsp70^{+} cells displayed higher levels of JNK with a high positive correlation between levels of JNK and Hsp70 signals in different *lgl^{-} yki^{OE}* clones (Fig. 5M). We also found that down-regulation of *hsp70A* group of transcripts in *lgl^{-} yki^{OE}* clones, which showed poor growth and transformation, also displayed reduced levels of p-JNK staining at 72hr ACI (Fig. 5N). Reduction in JNK signalling either by co-expression of *Ask^{RNAi}* transgene or the *Bsk^{DN}* allele too reduced levels of Hsp70 (Fig. 5O) and frequencies of *lgl^{-} yki^{OE}* clones (not shown).

Together, these results suggest that the hypoxic condition in niche areas near tracheae in larger *lgl^{-} yki^{OE}* clones activate JNK which activates dFOXO, leading subsequently to expression of Hsp70 in some cells in this niche.

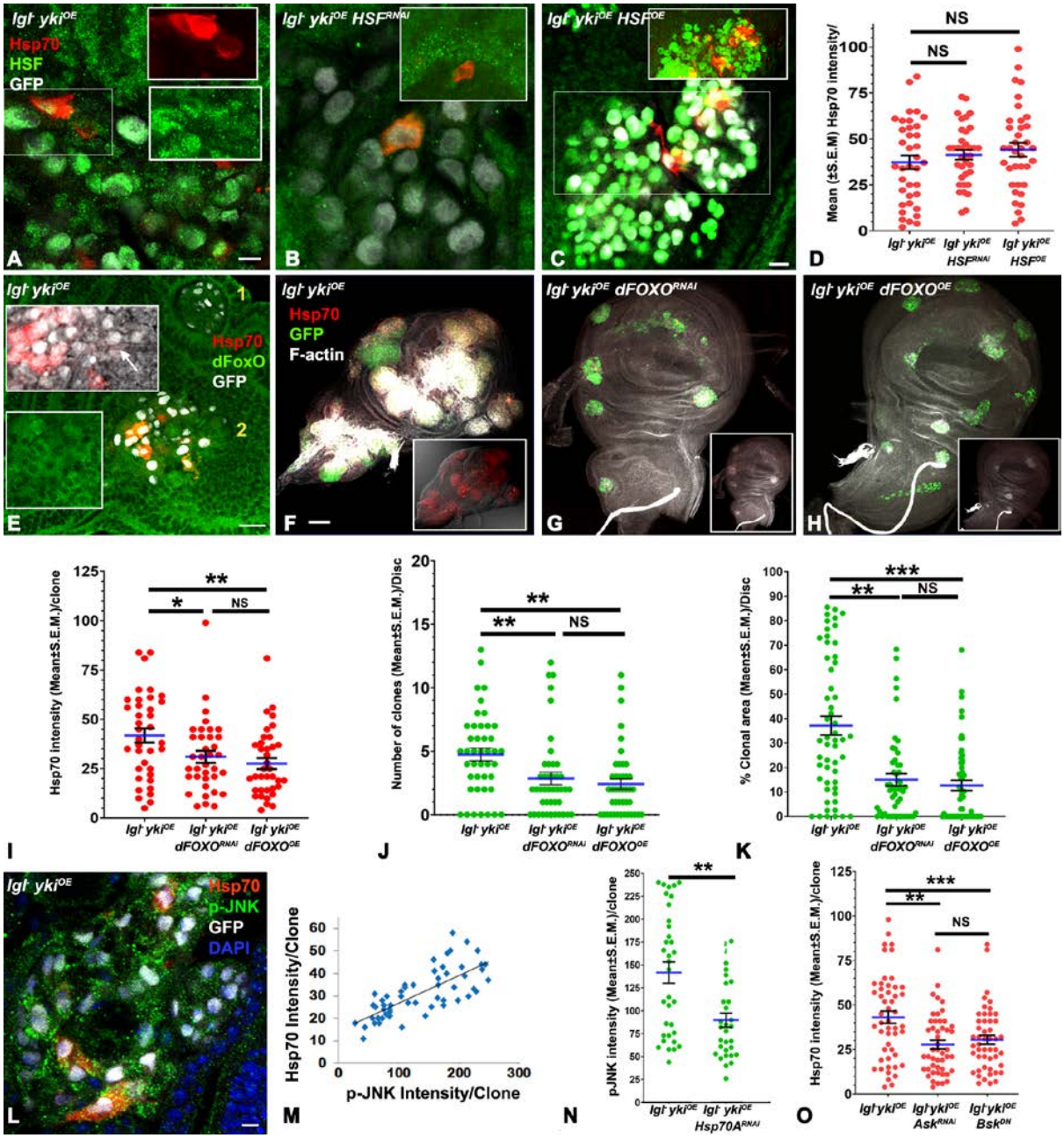

Fig 5 Perturbations in levels of dFOXO and JNK signalling, but not HSF, reduce Hsp70 expression in *lgl- yki^{OE}* clones and their growth. A-C: Confocal optical sections of wing imaginal discs at 72hr ACI showing distribution of Hsp70 (red) and HSF (green) in GFP positive (white) clones of different genotypes (noted at upper left corners); insets in **A** show Hsp70 (red) and HSF (green) staining, respectively, in the boxed area in **A**; insets in **B** and **C** show only Hsp70 (red) and HSF (green) at a lower magnification to more distinctly show the near complete absence and high levels of HSF in the clone area in **B** and **C**, respectively. **D:** Scatter plots of Hsp70 intensity/clone (Y-axis with Mean±S.E) of different genotypes (X-axis). **E:** Confocal projection image showing Hsp70 (red), dFOXO (green) in GFP (white) expressing *lgl- yki^{OE}* clones at 72hr ACI; **1** and **2** mark two clones without or with Hsp70 expressing cells, respectively; insets on left are part of the clone **2** to show Hsp70 (red) and DIC image (grey), and dFOXO (green, lower inset) expression, respectively; white arrow in the upper inset points to a tracheal branch traversing through the clone. **F-H:** Confocal projection images showing Hsp70 (red), GFP (green) and F-actin (white) staining in wing discs carrying clones of different

genotypes (noted on upper left corners) at 72hr ACI; insets in **F-H** are lower magnification images of the respective discs to show Hsp70 (red) and DIC (**F**) or Hsp70 and F-actin (white) staining against DIC background (grey, **G, H**). **I-K**: Scatter plot graphs showing Hsp70 fluorescence intensity per clone (**i**), numbers of clones per disc (**J**), and % Clonal Area per disc (Y-axis with Mean±S.E.) in different genotypes (X-axis). **L**: Optical section showing distribution of Hsp70 (red), p-JNK (green, in **L**), GFP (white) and DAPI (blue) in *lgl*$^{-}$ *yki*^{OE} clones at 72hr ACI. **M:** Correlation graph showing co-linearity between Hsp70 (Y-axis) and p-JNK (X-axis) intensity per *lgl*$^{-}$ *yki*^{OE} clone at 72hr ACI. **N** and **O:** Scatter-plot graphs showing p-JNK (**N**) and Hsp70 (**O**) intensity per clone (Y-axis with Mean±S.E.) in different genotypes (X axis) at 72hr ACI. In all scatter plot/bar graphs, the thick horizontal blue bar indicates the mean ±S.E.; the horizontal black lines on top indicate the pairs of scatter plots tested for statistical significance with the p-value indicated as: n.s. = >0.05, * =<0.05 and ** =<0.01. Scale bar in A = 5µm and applies to B, in C = 10µm, in E = 20µm, in F = 50µm and applies to G-H, in L = 20µm.

Different roles of HSF and dFOXO in *lgl*$^{-}$ *Ras*^{v12} tumorous clones in *Drosophila*

As noted above (Fig. 2), we found Hsp70 expression in epithelial tumours to be variable in relation to genetic background of the tumour cells. Therefore, we examined if the spatio-temporal expression of Hsp70 in *lgl*$^{-}$ *Ras*^{v12} clones followed same regulatory path as in *lgl*$^{-}$ *yki*^{OE} clones. Examination of effects of co-expression of *HSF*^{RNAi} or *HSF*^{OE} or *dFOXO*^{RNAi} transgene on growth of *lgl*$^{-}$ *Ras*^{v12} clones showed that compared to frequencies and sizes of *lgl*$^{-}$ *Ras*^{v12} clones at 48hr ACI (Fig. 6A), those co-expressing *HSF*^{RNAi} (Fig. 6B) were less frequent and smaller while those co-expressing *HSF*^{OE} (Fig. 6C) or *dFOXO*^{RNAi} (Fig. 6D) transgenes were more abundant and larger. The F-actin accumulation in these clones also varied accordingly (Fig. 6A-D). The scatter plots for clone frequencies and sizes shown in Fig. 6E and 6F confirm the above changes.

Immunostaining for Hsp70 in *lgl*$^{-}$ *Ras*^{v12} clones co-expressing *HSF*^{RNAi} or *HSF*^{OE} or *dFOXO*^{RNAi} transgenes (Fig. 6G-J) at 72hr ACI revealed that in parallel with the above changes in their growth patterns, the Hsp70 expression was substantially reduced in *lgl*$^{-}$ *Ras*^{v12} *HSF*^{RNAi} clones but greatly elevated in *lgl*$^{-}$ *Ras*^{v12} *HSF*^{OE}. On the other hand, the *lgl*$^{-}$ *Ras*^{v12} *dFOXO*^{RNAi} clones did not show appreciable change neither in Hsp70 expression nor in their growth (Fig. 6J).

These findings suggest that HSF and dFOXO have opposing roles in modulating growth of *lgl*$^{-}$ *yki*^{OE} and *lgl*$^{-}$ *Ras*^{v12} tumorous clones.

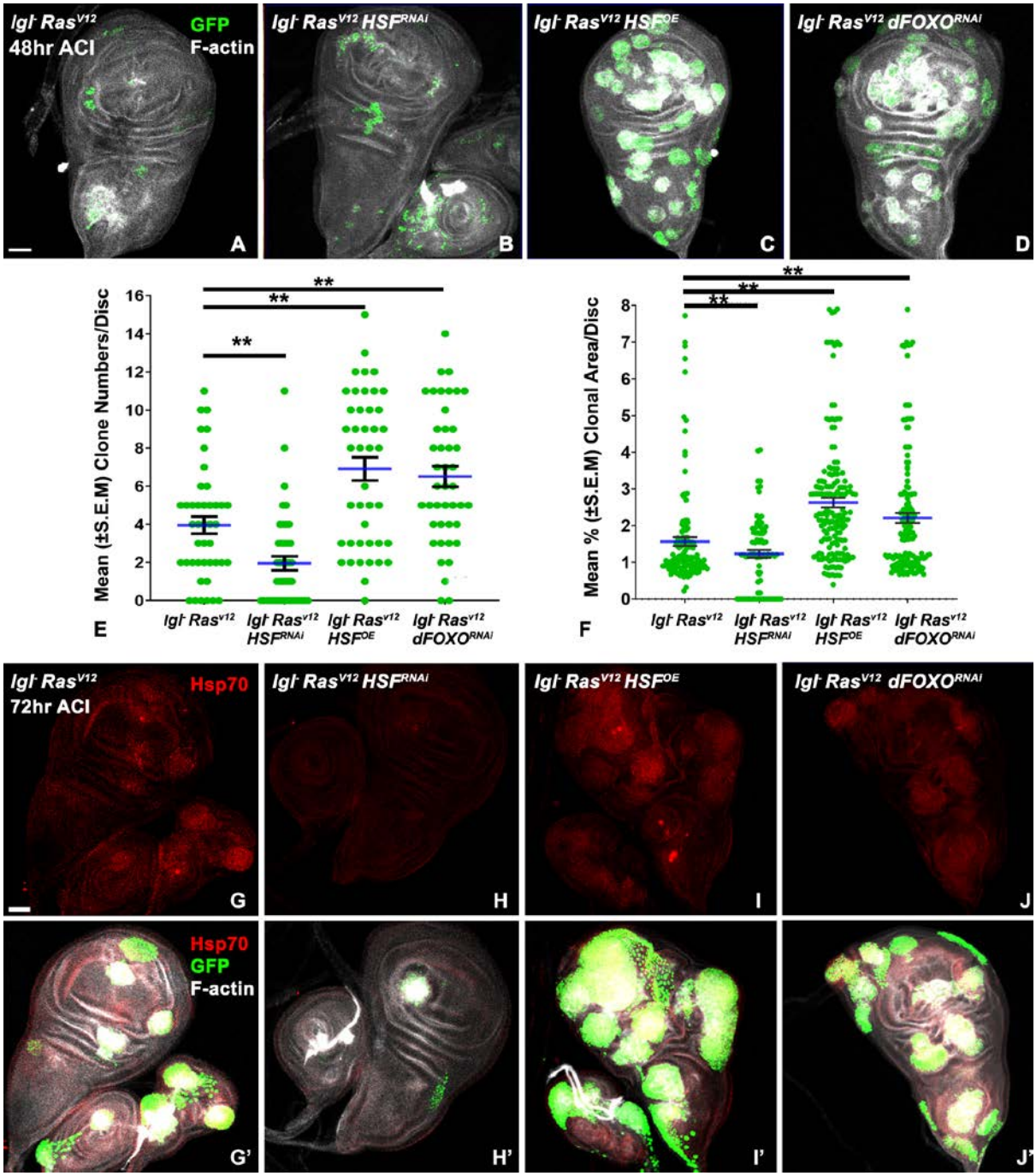

Fig. 6. HSF over-expression or dFoxo down-regulation increases neoplastic growth of *lgl- Ras^{v12}* clones. A-D': Confocal projection images of wing imaginal discs at 48hr ACI showing F-actin (white) and GFP (green) expressing clones of genotypes noted on left upper corners. **E-F:** Scatter plot graphs of Numbers of Clones/disc (**E**) or % Clonal area/per disc (**F**, Y-axis Mean±S.E) in different genotypes (X axis); the thick horizontal blue bars in the scatter plot/bar graphs indicate the mean while the thinner and shorter black bars indicate the ±S.E.M.; the horizontal black lines on top indicate the pairs of scatter plots tested for statistical significance with the p-value indicated as: n.s. = >0.05, * = <0.05 and ** = <0.01. **G-J':** Confocal projection images of wing imaginal discs at 72hr ACI showing distribution of Hsp70 (red) and F-actin (white) in GFP positive (green) clones of different genotypes (noted at upper left corners in **G-J**); images in **G-J** show only Hsp70 while those in **G'-J'** show merged staining for Hsp70,

GFP and F-actin in respective discs in **G-J**. Scale bars in A and G = 50µm and apply to B-D and G'-J', respectively.

Discussion

In our previous study (Singh et al., 2022) on temporal expression of Hsps during growth of *lgl*$^{-}$ tumours in presence of different tumour promoter environment, we noted that unlike the constitutively expressed Hsps, expression of stress-induced Hsp70 in these tumours followed an uniquely different spatial and temporal pattern. In the present study, we examined functional significance and regulation of the unique spatial and temporal expression of the stress-induced Hsp70 in epithelial tumours of different genetic backgrounds, with more detailed study on the *lgl*$^{-}$ *yki*^{OE} clonal tumours.

The very low frequency of tumorous *lgl*$^{-}$ *yki*^{OE} clonal cells expressing Hsp70 at early stage of tumorous clone's establishment (48hr ACI), but progressive increase thereafter implies specific role of Hsp70 in clonal cells as they progress to neoplastic stage. We found the time of appearance of the few Hsp70^{+} cells in *lgl*$^{-}$ *yki*^{OE} clones between 48hr and 72hr ACI to largely coincide with appearance of neoplastic transformation features, like F-actin nucleation, cytoplasmic protrusions and expression of mesenchymal markers like MMP1 and Ena (Gates et al., 2007; Lodge et al., 2021; Sano et al., 2012) indicating that these cells may be undergoing epithelial-mesenchymal transition (EMT). Coincidence of Hsp70 expression with neoplastic transformation was also evident in our finding that non-neoplastic *lgl*$^{-}$ MARCM clones or wing discs with non-malignant tumours associated with loss of polarity, as in *MS1096>lgl*^{RNAi} and *MS1096>Scrib*^{RNAi}, did not express the stress-inducible Hsp70 in any cell of the wing pouch, while all the genotypic conditions that generate malignant clonal tumours like *lgl*$^{-}$ *yki*^{OE} or *lgl*$^{-}$ *Ras*^{V12}, or tissue tumours like *MS1096>yki*^{Act} or *MS1096>Pvr*^{Act} or *Act>lgl*^{RNAi} or *MS1096>Ras*^{V12} *lgl*^{RNAi} or *MS1096>Ras*^{V12} *Scrib*^{RNAi} (Fig. 2, Table 1) showed Hsp70 expression, initially in a limited area which spread through the tumours as they got transformed. The stress inducible Hsp72 has been reported in malignant mouse mammary tumours also to be upregulated initially only in a few cancer initiating cells that show stem cell markers and undergo rapid metastasis (Gong et al., 2015). The observed absence of any impact of co-expression of *Hsp70A*^{RNAi} transgene in *lgl*$^{-}$ *yki*^{OE} clones in the early establishment of these clones (Fig. 1) agrees with the absence of Hsp70 protein during the early stages of clone establishment. However, the compromised growth and transformation of *lgl*$^{-}$ *yki*^{OE} clonal cells following down-regulation of Hsp70 expression through RNAi beyond 48hr ACI (Fig. 3),

strongly indicates that Hsp70 expression in some cells in the Lgl loss based epithelial tumours is critical for tracheoneogenesis in the growing tumours as well as their neoplasticity. It is notable that Hsp70 knockout mouse mammary tumours also displayed significantly reduced invasion and metastasis (Gong et al., 2015). The Hsp70 is known to be necessary for migration of border cells during oogenesis by modulating the dynamics of cytoskeletal components (Cobreros et al., 2008). Together, the Hsp70 appears to be a key factor in EMT and acquisition of invasive properties by loss of polarity associated malignant tumour cells in *Drosophila*.

It is interesting that co-expression of *hsp70B*^{RNAi} transgene did not have any detectable impact on survival of the host larvae. It is likely that the *hsp70B* group of genes are either not activated or these transcripts are not translated in *lgl*$^{-}$ *yki*^{OE} clonal cells. Our finding that unlike the presence of Hsp70 protein in only a few *lgl*$^{-}$ *yki*^{OE} clonal cells at 72hr ACI, the *hsp70* transcripts were present in all cells of these clones adds additional regulatory layers that impinge upon expression of this stress-inducible protein. A differential transcriptional activation of the two clusters of *hsp70* genes and translatability of their transcripts is known to operate under certain conditions (Lakhotia and Prasanth, 2002; Lakhotia et al., 2002; Singh and Lakhotia, 2016). In future studies, it will be interesting to examine possible regulatory role/s of the UTR regions of *hsp70A* and *hsp70B* gene clusters in regulating transcription and/or translation of the *hsp70* genes in *lgl*$^{-}$ *yki*^{OE} clones during their transformation and functional significance of such differential regulation, especially when their protein products are almost identical. It also remains to be examined if malignant tumours of other genetic backgrounds also differentially express the *hsp70* genes at the two clusters.

Our finding that over-expression of Hsp70 or its co-chaperone DnaJ (Hsp40) in all *lgl*$^{-}$ *yki*^{OE} clonal cells since the birth of a MARCM clone suppressed their establishment and growth is significant in the context of this protein's essential requirement for *lgl*$^{-}$ *yki*^{OE} clones' growth and transformation. Apparently, an elevated expression of the Hsp70 chaperone machinery at early stages of the clonal growth is deleterious. Overexpression of Hsp70 has been shown to inhibit responses downstream of plasma membrane receptors like the insulin receptor (Cobreros et al., 2008) or deleteriously affect cell survival (Krebs and Feder, 1997). In view of the high levels of Dcp-1 active caspase in the few *lgl*$^{-}$ *yki*^{OE} clones that survived till 48hr and 72hr ACI in Hsp70 or DnaJ over-expression background, we hypothesize that the targeted expression Hsp70 since birth of the *lgl*$^{-}$ *yki*^{OE} clone suppresses its establishment and growth because of the dominance of the pro-apoptotic role of Hsp70 (Lang et al., 2019; Radons, 2016).

This can explain why unlike the elevated expression of other heat shock proteins in *lgl*$^{-}$ *yki*^{OE} clones (Singh et al., 2022), the Hsp70 is kept silenced during early stages of tumour initiation and establishment.

High expression of markers like Sima, LDH, Gasp, and Tango in *lgl*$^{-}$ *yki*^{OE} clones suggests that, like the well-known neo-vascularization in mammalian cancers (Grifoni et al., 2015; Mirzoyan et al., 2019), tracheoneogenesis is induced as these growing tumours experience hypoxia. The spatial closeness of the few Hsp70^{+} cells in *lgl*$^{-}$ *yki*^{OE} clones at 48hr and 72hr ACI to tracheal branches suggests that the Hsp70 expression is related to the hypoxic niche. A role of hypoxia sensor Sima in inducing Hsp70 synthesis is indicated by our finding that over-expression of Sima in otherwise wild type background led to expression of Hsp70, which became stronger when *lgl*^{RNAi} was co-expressed. It is notable that Sima activity has been shown to be necessary for providing the invasive potential to epithelial cells in *Drosophila* (Doronkin et al., 2010). The initiation of Hsp70 expression in some tumorous cells located in the hypoxic niche with high F-actin nucleation thus indicates a causal relation between hypoxia, Hsp70 expression and transformation.

Studies on mammalian cancers have indicated that the hypoxia sensor, HIF-1a (mammalian homolog of *Drosophila* Sima) activates HSF which in turn causes elevated expression of Hsps in different mammalian cancer cells (Agarwal and Ganesh, 2020; Baird et al., 2006; Luo et al., 2021; Tsuchida et al., 2014). However, our earlier study on *lgl*$^{-}$ *yki*^{OE} clonal tumours in *Drosophila* (Singh et al., 2022) showed that their progression and transformation, and the expression of Hsp83 in them was HSF independent. The present results show that expression of the stress-inducible Hsp70 in *lgl*$^{-}$ *yki*^{OE} clonal tumours also does not depend upon HSF.

Presence of high dFOXO levels in the hypoxic niche where the Hsp70 expressing cells are located in *lgl*$^{-}$ *yki*^{OE} clones, and the significantly reduced Hsp70 levels and poor survival of the *lgl*$^{-}$ *yki*^{OE} clones with RNAi-dependent reduced dFOXO levels suggest that the dFoxo transcription factor has a direct role in Hsp70 expression in *lgl*$^{-}$ *yki*^{OE} tumorous clones. This agrees with recent studies that show dFOXO to regulate transcription of genes responding to oxidative stress, changes in cellular metabolism, and accumulation of unfolded proteins in *Drosophila* (Lim and Hyun, 2022; Puig et al., 2003; Wang et al., 2005; Zhang et al., 2016). Expression of dFOXO also promotes tolerance to hypoxia (Barretto et al., 2020). dFOXO-dependent expression of Hsps in response to stress has been demonstrated in *Drosophila* S2 cells (Donovan and Marr, 2016). The poor viability and growth of *lgl*$^{-}$ *yki*^{OE} clones in which

dFOXO was over-expressed appears to be a consequence of dFOXO-driven over-expression of Hsp70 during the initial stages of the tumorous clone establishment, which as discussed above adversely affects establishment and survival of *lgl*$^{-}$ *yki*^{OE} clones.

The high p-JNK level in the hypoxic niche where Hsp70^{+} cells are located agrees with the known (Donovan and Marr, 2016; Grifoni et al., 2015) elevation of p-JNK signaling following hypoxia. mouse embryonic stem cells show JNK dependent Hsp70 expression (Nishitai and Matsuoka, 2008). High JNK level is also known to be associated with mesenchymal and neoplastic cells (Muzzopappa et al., 2017; Uhlirova and Bohmann, 2006). Our observed positive correlation between p-JNK and Hsp70 levels in *lgl*$^{-}$ *yki*^{OE} clones and reduction in Hsp70 following down-regulation of p-JNK signaling by co-expression of *Ask*^{RNAi} or *Bask*^{DN} expression indicate critical roles of p-JNK signaling in expression of Hsp70 and transformation of *lgl*$^{-}$ *yki*^{OE} clones. This is further supported by the observed down-regulation of p-JNK levels in *Hsp70A*^{RNAi} co-expressing *lgl*$^{-}$ *yki*^{OE} clonal cells. Since *Hsp70A*^{RNAi} transgene expression leads to poor growth of these clones, they do not experience hypoxia, and consequently the p-JNK levels do not get elevated. Finally, since hypoxia and high p-JNK induce dFOXO (Barretto et al., 2020; Donovan and Marr, 2016), we hypothesize that as the *lgl*$^{-}$ *yki*^{OE} clones grow, some cells experience greater hypoxic stress and thus acquire higher levels of p-JNK, which leads to induction of Hsp70 via dFOXO.

Our finding that unlike the presence of Hsp70 protein in only a few *lgl*$^{-}$ *yki*^{OE} clonal cells at 72hr ACI, the *hsp70* transcripts were present in all cells of these clones adds additional regulatory layers that impinge upon expression of this stress-inducible protein. It is known that under certain conditions, the stress-induced transcription of *hsp70* genes and translation of the generated mRNAs can be temporally dissociated (Lakhotia and Prasanth, 2002; Lakhotia et al., 2002; Singh and Lakhotia, 2016). Mechanism and functional significance of such regulatory layers remain to be understood. It will be interesting to examine roles of Yorkie-Bantam-mTOR-Akt interacting network in regulating the cap-independent translation (Sun et al., 2011; Ye et al., 2012) in selective synthesis of Hsp70 in a few cells of the tumorous clones.

An unexpected but significant of our study is that the generally similar spatio-temporal pattern of Hsp70 expression in *lgl*$^{-}$ *yki*^{OE} and *lgl*$^{-}$ *Ras*^{v12} tumorous clones is dependent upon opposing roles of HSF and dFOXO Involvement of HSF in inducing Hsp70 expression in the established *lgl*$^{-}$ *Ras*^{v12} clones seen in our study parallels the role of HSF in activating Hsp genes, including Hsp70 in Ras dependent human tumours (Dai et al., 2007; Mendillo et al., 2012). Such

differences between the *lgl⁻ yki^OE* and *lgl⁻ Ras^V12* clones may be related to the opposing roles of Ras and Yorkie in senescence and growth, respectively (Ito and Igaki, 2021). This aspect needs further studies. It will be also interesting to examine if dFOXO is involved in expression of stress-induced Hsp70 in the Hippo/Yorkie-signalling dependent mammalian cancers.

In addition to the slower growth of *lgl⁻ Ras^v12* clones than of the *lgl⁻ yki^OE* clones (Singh et al., 2022), the frequencies of Hsp70 expressing cells at 72hr ACI in these two types of tumorous clones also differed. In this context, it is interesting to note that the aggressively growing tumours like *lgl⁻ yki^OE*, *Act>lgl^RNAi*, *MS1096>yki^Act*, *MS1096>Pvr^Act MS1096> yki^Act* showed more abundant Hsp70 expression than the slower growing *MS1096>Ras^v12 lgl^RNAi* or *MS1096>Ras^v12 Scrib^RNAi* tumours of similar stage. It will be interesting to examine roles of HSF and dFoxo in expression of Hsp70 in tumours of such different genetic backgrounds.

Taken together, present studies suggest that the expression of the stress-inducible Hsp70 in only a few cells in a clone relates to the micro-heterogeneity existing between different cells comprising a tumourigenic clone and that this protein has a major role in acquisition of neoplastic features. Our finding that tumours having different genetic aetiology exploit different regulatory circuits to activate Hsp70 to get transformed has implications for developing efficient therapeutic approaches for diverse human cancers. The powerful tools available in fly genetics will be very useful to understand the diverse pathways that modulate establishment and transformation of tumours of different etiology and genetic background.

Materials and Methods

Fly stocks and genetics

All fly stocks and crosses were maintained on standard agar-maize powder, yeast and sugar food at 24 ± 1 °C (Chaudhuri et al 2021). The following fly stocks were used to set up crosses to obtain progeny of the desired genotypes: 1. *w*; lgl^4 FRT40A/CyO; Sb/TM6B* (*lgl^4* is referred to as *lgl⁻*); 2. *y w* hsFLP; FRT40A w⁺ y⁺/CyO-GFP*; 3. *y w* hsFLP tubGAL4 UAS-GFP; tubGAL80 FRT40A/CyO-GFP; +/+*; 4. *w*; lgl⁻ FRT40A UAS-yki /CyO-GFP*; +/+ (*UAS-yki* referred to as *yki^OE*); 5. *w*; lgl⁻ FRT40A UAS-Ras^V12/CyO-GFP* (*UAS-Ras^V12* referred to as *Ras^v12*); 6. *MS1096-GAL4; +/+; +/+* (Capdevila and Guerrero, 1994); 7. *w*; +/+; UAS-yki^Act* (BDSC-28817; referred to as *yki^Act*); 9. *y^1 v^1; UAS-HSF-RNAi/TM3, Sb^1* (BDSC-27070, referred to as *HSF^RNAi*); 12. *y^1 v^1; UAS-HSF-eGFP*; referred to as *HSF^OE*); 13. *y 1 sc* v 1 sev21; P{y[+t7.7] v[+t1.8]=TRiP.GLV31035}attP2* (BDSC-33661); 14. *y 1 sc* v 1 sev21; P{y[+t7.7]*

v[+t1.8]=TRiP.GLV21028}attP2 (BDSC-35663; referred to as $Hsp70A^{RNAi}$ as it targets the *hsp70Aa* and *hsp70Ab* genes present at 87A locus); 15. *y 1 v 1 ; P{y[+t7.7] v[+t1.8]=TRiP.JF03215}attP2* (BDSC-28787; referred to as $hsp70B^{RNAi}$ as it targets the hsp70*Ba*, *hsp70Bb*, *hsp70Bbb* and *hsp70Bbc* genes present at the 87C locus); 16. w^{1118}*; +/+; UAS-Hsp70 #4.4* (Xiao et al., 2007)*;* this transgene, located on chromosome 3 is referred to as $Hsp70A^{OE}$; 17. *sc[*] v [1] sev[21]; P{y[+t7.7]v[+t1.8]=TRiP.HMS00793}attP2* (BDSC-32993, referred to as $dFOXO^{RNAi}$)*;*18. w^{118}*; +/+; UAS-dFoxo,* referred to as $dFOXO^{OE}$*;* 19. *w*; P{w[+mCJ=UAS-DnaJ-1.K}3* (BDSC-30553): In this line, the P{w[+mCJ=UAS-DnaJ-1.K}3 transgene is inserted on chromosome 3 and over-express DnaJ under UAS control. This transgene is referred to as $DnaJ^{OE}$.

The stocks 1-6 above were provided by Prof. Pradip Sinha (IIT Kanpur, India; see (Khan et al., 2013), 13 by Prof. J.T. Lis, USA, 16 by Dr. C. Xiao, Canada (Xiao et al., 2007), 18 by Prof. Maria Leptin, Germany while others were either available in our laboratory or were obtained from the Bloomington Drosophila Stock Centre (BDSC).

Generation of tumours in imaginal discs

As described earlier (Singh et al., 2022), epithelial tumours in larval wing imaginal discs were generated either using the MARCM (Mosaic Analysis with a Repressible Cell Marker) technique or driving expression of the desired *UAS* carrying tumour inducing transgene in the wing pouch region (Capdevila and Guerrero, 1994) with *MS1096-GAL4* driver, or ubiquitously in all body cells with the *Act5C-GAL4* (Yepiskoposyan et al., 2006).

Using the above listed stocks, males of appropriate genotypes were crossed with virgin flies from the MARCM stock (*y w hsFLP tubGAL4 UAS-GFP; FRT40A GAL80/CyO-GFP; +/+*) to obtain progenies of the following genotypes either to generate lgl^{-} MARCM clones co-expressing the desired transgene/mutant allele or to generate tumours of different genotypes in the larva wing discs. The lgl^{-} yki^{OE} or $lgl^{-}Ras^{V12}$ MARCM clones were generated by a 3 or 5 min 37^{o}C heat shock, respectively, to early third instar larvae (72hr after egg laying or 72hr AEL) and clone age expressed as hours after clone induction (hr ACI) as described earlier (Singh et al., 2022). Using this strategy, progenies of the following genotypes, carrying lgl^{-} clones in combination with the other transgenes, were examined.

1. *y w hsFLP tubGAL4 UAS-GFP; tubGAL80 FRT40A/*lgl^{-} *FRT40A; +/+*

2. *y w hsFLP tubGAL4 UAS-GFP; tubGAL80 FRT40A/lgl^{-} FRT40A; mCD8^{GFP}*

3. *y w hsFLP tubGAL4 UAS-GFP; tubGAL80 FRT40A/lgl^{-} FRT40A; HSF$^{GFP\text{-}OE}$*

4. *y w hsFLP tubGAL4 UAS-GFP; tubGAL80 FRT40A/lgl^{-} FRT40A; Hsp70A^{OE}/+*

lgl^{-} yki^{OE} clones

5. *y w hsFLP tubGAL4 UAS-GFP; tubGAL80 FRT40A/lgl^{-} yki^{OE} FRT40A; +/+*

6. *y w hsFLP tubGAL4 UAS-GFP; tubGAL80 FRT40A/lgl^{-} yki^{OE} FRT40A; Hsp70A^{RNAi}*

7. *y w hsFLP tubGAL4 UAS-GFP; tubGAL80 FRT40A/lgl^{-} yki^{OE} FRT40A; Hsp70A^{OE}*

8. *y w hsFLP tubGAL4 UAS-GFP; tubGAL80 FRT40A/lgl^{-} yki^{OE} FRT40A; Hsp70B^{RNAi}*

9. *y w hsFLP tubGAL4 UAS-GFP; tubGAL80 FRT40A/lgl^{-} yki^{OE} FRT40A; DnaJ^{OE}*

10. *y w hsFLP tubGAL4 UAS-GFP; tubGAL80 FRT40A/lgl^{-} FRT40A; dFOXO^{OE}/+*

11. *y w hsFLP tubGAL4 UAS-GFP; tubGAL80 FRT40A/lgl^{-} FRT40A; dFOXO^{RNAi}/+*

12. *y w hsFLP tubGAL4 UAS-GFP; tubGAL80 FRT40A/lgl^{-} yki^{OE} FRT40A; HSF^{RNAi}/+*

13. *y w hsFLP tubGAL4 UAS-GFP; tubGAL80 FRT40A/lgl^{-} yki^{OE} FRT40A; HSF^{OE}/+*

14. *y w hsFLP tubGAL4 UAS-GFP; tubGAL80 FRT40A/lgl^{-} yki^{OE} FRT40A; Ask^{RNAi}/+*

15. *y w hsFLP tubGAL4 UAS-GFP; tubGAL80 FRT40A/lgl^{-} yki^{OE} FRT40A; ND75^{RNAi}/+*

16. *y w hsFLP tubGAL4 UAS-GFP; tubGAL80 FRT40A/lgl^{-} yki^{OE} FRT40A; Bsk^{DN}/+*

17. *y w hsFLP tubGAL4 UAS-GFP; tubGAL80 FRT40A/lgl^{-} yki^{OE} FRT40A; LDH^{LacZ}/+*

lgl^{-} Ras^{V12} clones

18. *y w hsFLP tubGAL4 UAS-GFP; tubGAL80 FRT40A/lgl^{-} Ras^{V12} FRT40A; +/+*

19. *y w hsFLP tubGAL4 UAS-GFP; tubGAL80 FRT40A/lgl^{-} Ras^{V12} FRT40A; dFOXO^{OE}/+*

20. *y w hsFLP tubGAL4 UAS-GFP; tubGAL80 FRT40A/lgl^{-} Ras^{V12} FRT40A; dFOXO^{RNAi}/+*

21. *y w hsFLP tubGAL4 UAS-GFP; tubGAL80 FRT40A/lgl^{-} Ras^{V12} FRT40A; HSF^{RNAi}/+*

22. *y w hsFLP tubGAL4 UAS-GFP; tubGAL80 FRT40A/lgl^{-} Ras^{V12} FRT40A; HSF^{OE}/+*

Progenies of the following genotypes that resulted in epithelial tumors in wing discs were also obtained through appropriate crosses.

1. *MS1096>lgl^{RNAi}*
2. *MS1096>Ras^{v12} lgl^{RNAi}*
3. *MS1096>*Scrib^{RNAi}
4. *MS1096>Ras^{v12}* Scrib^{RNAi}
5. *MS1096>Sima^{OE} lgl^{RNAi}*
6. *Act>lgl^{RNAi}*

Survival assay

In order to study the effect of tumorous clones on survival of the host, larvae of the desired genotypes were allowed to grow at 24°C till emergence of adults. Numbers of those dying at early pupal (psuedopupae) or late pupal (pharate) stages and adults that emerged were counted. Different data sets were compared with Student's t-Test for statistical significance using Sigma plot Software.

Immunostaining

Imaginal discs were dissected out in Poels' salt solution (Tapadia and Lakhotia, 1997) from third instar larvae of the desired genotypes and age (hr ACI in case of MARCM clones and days (after egg laying) for *MS1096-GAL4* or *Act-GAL4* driven epithelial tumours), and processed for immunostaining as described earlier (Ray et al., 2019). The primary antibodies used were: 1. Anti-Hsp70 (7Fb, gift by Dr. M. B. Evgen'ev; 1:200 dilution) raised in rat, which detects only the stress inducible *Drosophila* Hsp70 (Velazquez and Lindquist, 1984); 2. Anti-cleaved Caspase-3 (Cell Signalling, Asp-216, 1:100 dilution); 3. Anti-MMP1 (DSHB-5H7B11, 1:100 dilution); 4. Anti-HSF (gift by Prof. J. T. Lis, 1:300 dilution); 5. Anti-dFOXO (gift by Dr. P Wappner, Germany, 1:50 dilution); 6. Anti-LacZ (Abcam ab9361, 1:500 dilution); 7. Anti-p-JNK (pTPpY, Promega, USA-1:100 dilution); 8. Anti-Sima (gift by Dr. P. Wappner,

Germany, 1:100 dilution). Appropriate secondary antibodies conjugated either with Cy3 (1:200 dilution, Sigma-Aldrich, India) or Alexa Fluor 546 (1:200 dilution; Molecular Probes, USA) were used to detect the given primary antibody. Phalloidin-633 (#A22284, Invitrogen) and 6-diamidino-2-phenylindole dihydrochloride (DAPI, 1 μg/ml) were used to stain F-Actin and DNA, respectively. The immunostained tissues were mounted in 1,4-Diazabicyclo [2.2.2] octane (DABCO) antifade mountant for confocal microscopy with Zeiss LSM Meta 510 system using Plan-Apo 20X (0.8 NA), 40X (1.3 NA) or 63X (1.4 NA) oil immersion objectives and Zeiss ZEN software. Quantitative estimates of proteins in different regions of wing disc or eye discs were obtained using the Histo or Profile option of ZEN (Blue) software. Images in all illustrations shown here were assembled using the Adobe Photoshop 7.0. Significance testing between the data for control and experimental genotypes was performed with the Mann–Whitney U-test or Chi-squared test using GraphPad Prism 8.4.3.

Fluorescent RNA in situ hybridisation (FRISH)

Imaginal discs from third instar larvae carrying *lgl*$^{-}$ *yki*^{OE} MARCM clones (72hr ACI) were dissected out in 1xPBS and fixed in 4% formaldehyde as described above for immunostaining. The fixed discs were processed for FRISH using a 5'-Cy3-tagged single strand oligonucleotide probe (Integrated DNA Technologies, BVBA, Belgium), TCACTTTAACTTGCACTTTACTGCAGATTGTTTAGCTTGTT, which hybridizes with 5' UTR of all the *hsp70* genes in *Drosophila melanogaster*, essentially following the procedure described earlier (Singh et al., 2019). After the in situ hybridization, the discs were processed for immunostaining with the anti-Hsp70 7Fb antibody as described above. Discs were finally counterstained with DAPI, mounted in DABCO and examined with Zeiss LSM Meta 510 system using 40X (1.3 NA) or 63X (1.4 NA) oil immersion objectives and Zeiss ZEN software.

Acknowledgements: GS thanks the University Grants Commission (New Delhi) and Council of Scientific & Industrial Research (N. Delhi) for research fellowship. SCL acknowledges the Science & Engineering Research Board (Govt. of India) for the Distinguished Fellowship. We thank Dr. Pradip Sinha (India), Dr. J. T. Lis (USA), Dr. C. Xiao (Canada), Dr. Maria Leptin (Germany) and the Bloomington Drosophila Stock Centre (USA) for sharing the fly stocks as listed in Materials and Methods, and Dr. J. T. Lis (USA), Dr. P. Wappner (Germany), and Dr. M. B. Evgen'ev (Russia) for generously sharing different primary antibodies, as noted in Materials and Methods. We also thank Dr. Anand K. Singh (India) for providing the Cy3-tagged *hsp70* oligo probe and help with FRISH.

Competing interests: None

Funding: Department of Biotechnology (Govt. of India) Grant no. BT/PR14716/BRB/10/876/2010.

6. References

Agarwal, S. and Ganesh, S. (2020). Perinuclear mitochondrial clustering, increased ROS levels, and HIF1 are required for the activation of HSF1 by heat stress. *J Cell Sci* **133**.

Arya, R., Mallik, M. and Lakhotia, S. C. (2007). Heat shock genes - integrating cell survival and death. *J Biosci* **32**, 595-610.

Baird, N. A., Turnbull, D. W. and Johnson, E. A. (2006). Induction of the heat shock pathway during hypoxia requires regulation of heat shock factor by hypoxia-inducible factor-1. *J Biol Chem* **281**, 38675-81.

Barretto, E. C., Polan, D. M., Beevor-Potts, A. N., Lee, B. and Grewal, S. S. (2020). Tolerance to hypoxia is promoted by FOXO regulation of the innate immunity transcription factor NF-κB/Relish in *Drosophila*. *Genetics* **215**, 1013-1025.

Bukau, B., Deuerling, E., Pfund, C. and Craig, E. A. (2000). Getting newly synthesized proteins into shape. *Cell* **101**, 119-22.

Bunker, B. D., Nellimoottil, T. T., Boileau, R. M., Classen, A. K. and Bilder, D. (2015). The transcriptional response to tumorigenic polarity loss in Drosophila. *Elife* **4**.

Calleja, M., Morata, G. and Casanova, J. (2016). Tumorigenic Properties of Drosophila Epithelial Cells Mutant for lethal giant larvae. *Dev Dyn* **245**, 834-43.

Capdevila, J. and Guerrero, I. (1994). Targeted expression of the signaling molecule decapentaplegic induces pattern duplications and growth alterations in Drosophila wings. *EMBO journal* **13**, 4459-4468.

Chang, Y. W., Sun, Y. J., Wang, C. and Hsiao, C. D. (2008). Crystal structures of the 70-kDa heat shock proteins in domain disjoining conformation. *J Biol Chem* **283**, 15502-11.

Cobreros, L., Fernández-Miñán, A., Luque, C. M., González-Reyes, A. and Martín-Bermudo, M. D. (2008). A role for the chaperone Hsp70 in the regulation of border cell migration in the Drosophila ovary. *Mechanisms of Development* **125**, 1048-1058.

Cyran, A. M. and Zhitkovich, A. (2022). Heat shock proteins and HSF1 in cancer. *Frontiers in oncology* **12**, 860320.

Dai, C., Whitesell, L., Rogers, A. B. and Lindquist, S. (2007). Heat shock factor 1 Is a powerful multifaceted modifier of carcinogenesis. *Cell* **130**, 1005-1018.

Daugaard, M., Rohde, M. and Jäättelä, M. (2007). The heat shock protein 70 family: Highly homologous proteins with overlapping and distinct functions. *FEBS Lett* **581**, 3702-10.

Donovan, M. R. and Marr, M. T. (2016). dFOXO activates large and small heat shock protein genes in response to oxidative stress to maintain proteostasis in *Drosophila**. *Journal of Biological Chemistry* **291**, 19042-19050.

Doronkin, S., Djagaeva, I., Nagle, M. E., Reiter, L. T. and Seagroves, T. N. (2010). Dose-dependent modulation of HIF-1α/sima controls the rate of cell migration and invasion in Drosophila ovary border cells. *Oncogene* **29**, 1123-1134.

Feige, U. and Polla, B. S. (1994). Hsp70--a multi-gene, multi-structure, multi-function family with potential clinical applications. *Experientia* **50**, 979-86.

Flaherty, K. M., DeLuca-Flaherty, C. and McKay, D. B. (1990). Three-dimensional structure of the ATPase fragment of a 70K heat-shock cognate protein. *Nature* **346**, 623-8.

Gates, J., Mahaffey, J. P., Rogers, S. L., Emerson, M., Rogers, E. M., Sottile, S. L., Van Vactor, D., Gertler, F. B. and Peifer, M. (2007). Enabled plays key roles in embryonic epithelial morphogenesis in Drosophila. *Development* **134**, 2027-39.

Gong, J., Weng, D., Eguchi, T., Murshid, A., Sherman, M. Y., Song, B. and Calderwood, S. K. (2015). Targeting the hsp70 gene delays mammary tumor initiation and inhibits tumor cell metastasis. *Oncogene* **34**, 5460-5471.

Grifoni, D., Sollazzo, M., Fontana, E., Froldi, F. and Pession, A. (2015). Multiple strategies of oxygen supply in Drosophila malignancies identify tracheogenesis as a novel cancer hallmark. *Sci Rep* **5**, 9061.

Ish-Horowicz, D., Pinchin, S. M., Gausz, J., Gyurkovics, H., Bencze, G., Goldschmidt-Clermont, M. and Holden, J. J. (1979). Deletion mapping of two D. melanogaster loci that code for the 70,000 dalton heat-induced protein. *Cell* **17**, 565-71.

Ito, T. and Igaki, T. (2021). Yorkie drives Ras-induced tumor progression by microRNA-mediated inhibition of cellular senescence. *Sci Signal* **14**.

Jiramongkol, Y. and Lam, E. W. F. (2020). FOXO transcription factor family in cancer and metastasis. *Cancer and Metastasis Reviews* **39**, 681-709.

Juhasz, K., Lipp, A. M., Nimmervoll, B., Sonnleitner, A., Hesse, J., Haselgruebler, T. and Balogi, Z. (2013). The complex function of hsp70 in metastatic cancer. *Cancers (Basel)* **6**, 42-66.

Khan, S., Bajpai, A., Alam, M., Gupta, R., Harsh, S., Pandey, R., Goel-Bhattacharya, S., Nigam, A., Mishra, A. and Sinha, P. (2013). Epithelial neoplasia in Drosophila entails switch to primitive cell states. *Proc Natl Acad Sci USA* **110**, E2163–E2172.

Krebs, R. A. and Feder, M. E. (1997). Tissue-specific variation in Hsp70 expression and thermal damage in Drosophila melanogaster larvae. *J Exp Biol* **200**, 2007-15.

Lakhotia, S. C. and Prasanth, K. V. (2002). Tissue- and development-specific induction and turnover of hsp70 transcripts from loci 87A and 87C after heat shock and during recovery in Drosophila melanogaster. *J Exp Biol* **205**, 345-58.

Lakhotia, S. C., Srivastava, P. and Prasanth, K. V. (2002). Regulation of heat shock proteins, Hsp70 and Hsp64, in heat-shocked Malpighian tubules of Drosophila melanogaster larvae. *Cell Stress Chaperones* **7**, 347-56.

Lang, B. J., Guerrero-Giménez, M. E., Prince, T. L., Ackerman, A., Bonorino, C. and Calderwood, S. K. (2019). Heat shock proteins are essential components in transformation and tumor progression: cancer cell intrinsic pathways and beyond. *Int J Mol Sci* **20**.

Leu, J. I., Pimkina, J., Pandey, P., Murphy, M. E. and George, D. L. (2011). HSP70 inhibition by the small-molecule 2-phenylethynesulfonamide impairs protein clearance pathways in tumor cells. *Mol Cancer Res* **9**, 936-47.

Li, J., Han, S., Li, H., Udeshi, N. D., Svinkina, T., Mani, D. R., Xu, C., Guajardo, R., Xie, Q., Li, T. et al. (2020). Cell-surface proteomic profiling in the fly brain uncovers wiring regulators. *Cell* **180**, 373-386.e15.

Lim, J. J. and Hyun, S. (2022). Minocycline treatment improves proteostasis during Drosophila aging via autophagy mediated by FOXO and Hsp70. *Biomedicine & Pharmacotherapy* **149**, 112803.

Lodge, W., Zavortink, M., Golenkina, S., Froldi, F., Dark, C., Cheung, S., Parker, B. L., Blazev, R., Bakopoulos, D., Christie, E. L. et al. (2021). Tumor-derived MMPs regulate cachexia in a Drosophila cancer model. *Dev Cell* **56**, 2664-2680.e6.

Luo, S. Y., Wang, J. Q., Liu, C., Gao, X. M., Zhang, Y. B., Ding, J., Hou, C. C., Zhu, J. Q., Lou, B., Shen, W. L. et al. (2021). Hif-1α/Hsf1/Hsp70 signaling pathway regulates redox homeostasis and apoptosis in large yellow croaker (Larimichthys crocea) under environmental hypoxia. *Zool Res* **42**, 746-760.

Masser, A. E., Ciccarelli, M. and Andr´easson, l. (2020). Hsf1 on a leash – controlling the heat shock response by chaperone titration. *Experimental Cell Research* **396**, 112246.

Medioni, C., Sénatore, S., Salmand, P. A., Lalevée, N., Perrin, L. and Sémériva, M. (2009). The fabulous destiny of the Drosophila heart. *Curr Opin Genet Dev* **19**, 518-25.

Mendillo, Marc L., Santagata, S., Koeva, M., Bell, George W., Hu, R., Tamimi, Rulla M., Fraenkel, E., Ince, Tan A., Whitesell, L. and Lindquist, S. (2012). HSF1 drives a transcriptional program distinct from heat shock to support highly malignant human cancers. *Cell* **150**, 549-562.

Mirzoyan, Z., Sollazzo, M., Allocca, M., Valenza, A. M., Grifoni, D. and Bellosta, P. (2019). Drosophila melanogaster: A Model Organism to Study Cancer. *Front Genet* **10**, 51.

Morimoto, R. I. (1998). Regulation of the heat shock transcriptional response: cross talk between a family of heat shock factors, molecular chaperones, and negative regulators. *Genes Dev* **12**, 3788-96.

Murphy, M. E. (2013). The HSP70 family and cancer. *Carcinogenesis* **34**, 1181-8.

Muzzopappa, M., Murcia, L. and Milán, M. (2017). Feedback amplification loop drives malignant growth in epithelial tissues. *Proc Natl Acad Sci U S A* **114**, E7291-e7300.

Nishitai, G. and Matsuoka, M. (2008). Differential regulation of HSP70 expression by the JNK kinases SEK1 and MKK7 in mouse embryonic stem cells treated with cadmium. *Journal of Cellular Biochemistry* **104**, 1771-1780.

Puig, O., Marr, M. T., Ruhf, M. L. and Tjian, R. (2003). Control of cell number by Drosophila FOXO: downstream and feedback regulation of the insulin receptor pathway. *Genes & development* **17**, 2006-2020.

Radons, J. (2016). The human HSP70 family of chaperones: where do we stand? *Cell Stress Chaperones* **21**, 379-404.

Ray, M., Singh, G. and Lakhotia, S. C. (2019). Altered levels of hsromega lncRNAs further enhance Ras signaling during ectopically activated Ras induced R7 differentiation in Drosophila. *Gene Expr Patterns* **33**, 20-36.

Sano, H., Kunwar, P. S., Renault, A. D., Barbosa, V., Clark, I. B., Ishihara, S., Sugimura, K. and Lehmann, R. (2012). The Drosophila actin regulator ENABLED regulates cell shape and orientation during gonad morphogenesis. *PLoS One* **7**, e52649.

Sansone, C. L. and Blumenthal, E. M. (2013). Neurodegeneration in drop-dead mutant drosophila melanogaster is associated with the respiratory system but not with Hypoxia. *PLoS One* **8**, e68032.

Sarge, K. D., Murphy, S. P. and Morimoto, R. I. (1993). Activation of heat shock gene transcription by heat shock factor 1 involves oligomerization, acquisition of DNA-binding activity, and nuclear localization and can occur in the absence of stress. *Mol Cell Biol* **13**, 1392-407.

Singh, A. K., Choudhury, S. R., De, S., Zhang, J., Kissane, S., Dwivedi, V., Ramanathan, P., Petric, M., Orsini, L., Hebenstreit, D. et al. (2019). The RNA helicase UPF1 associates with mRNAs co-transcriptionally and is required for the release of mRNAs from gene loci. *eLife* **8**, e41444.

Singh, A. K. and Lakhotia, S. C. (2016). Expression of hsrω-RNAi transgene prior to heat shock specifically compromises accumulation of heat shock-induced Hsp70 in Drosophila melanogaster. *Cell Stress Chaperones* **21**, 105-120.

Singh, G., Chakraborty, S. and Lakhotia, S. C. (2022). Elevation of major constitutive heat shock proteins is heat shock factor independent and essential for establishment and growth of Lgl loss and Yorkie gain-mediated tumors in Drosophila. *bioRxiv*, 2021.08.30.458144.

Sonnenfeld, M., Ward, M., Nystrom, G., Mosher, J., Stahl, S. and Crews, S. (1997). The Drosophila tango gene encodes a bHLH-PAS protein that is orthologous to mammalian Arnt and controls CNS midline and tracheal development. *Development* **124**, 4571-82.

Stankiewicz, A. R., Lachapelle, G., Foo, C. P., Radicioni, S. M. and Mosser, D. D. (2005). Hsp70 inhibits heat-induced apoptosis upstream of mitochondria by preventing Bax translocation. *J Biol Chem* **280**, 38729-39.

Sun, J., Conn, C. S., Han, Y., Yeung, V. and Qian, S.-B. (2011). PI3K-mTORC1 attenuates stress response by inhibiting cap-independent Hsp70 translation. *J Biol Chem* **286**, 6791-6800.

Tafesh-Edwards, G. and Eleftherianos, I. (2020). JNK signaling in Drosophila immunity and homeostasis. *Immunology Letters* **226**, 7-11.

Tamori, Y., Suzuki, E. and Deng, W. M. (2016). Epithelial Tumors Originate in Tumor Hotspots, a Tissue-Intrinsic Microenvironment. *PLoS Biol* **14**, e1002537.

Tapadia, M. and Lakhotia, S. (1997). Specific induction of the hsr omega locus of Drosophila melanogaster by amides. *Chromosome Research* **5**, 359-362.

Tsarouhas, V., Senti, K. A., Jayaram, S. A., Tiklová, K., Hemphälä, J., Adler, J. and Samakovlis, C. (2007). Sequential pulses of apical epithelial secretion and endocytosis drive airway maturation in Drosophila. *Dev Cell* **13**, 214-25.

Tsuchida, S., Arai, Y., Takahashi, K. A., Kishida, T., Terauchi, R., Honjo, K., Nakagawa, S., Inoue, H., Ikoma, K., Ueshima, K. et al. (2014). HIF-1α-induced HSP70 regulates anabolic responses in articular chondrocytes under hypoxic conditions. *J Orthop Res* **32**, 975-80.

Uhlirova, M. and Bohmann, D. (2006). JNK- and Fos-regulated Mmp1 expression cooperates with Ras to induce invasive tumors in Drosophila. *Embo j* **25**, 5294-304.

Vasan, N., Baselga, J. and Hyman, D. M. (2019). A view on drug resistance in cancer. *Nature* **575**, 299-309.

Velazquez, J. M. and Lindquist, S. (1984). hsp70: nuclear concentration during environmental stress and cytoplasmic storage during recovery. *Cell* **36**, 655-62.

Wang, M. C., Bohmann, D. and Jasper, H. (2005). JNK extends life span and limits growth by antagonizing cellular and organism-wide responses to insulin signaling. *Cell* **121**, 115-125.

Wu, C. (1995). Heat shock transcription factors: Structure and regulation. *Annu. Rev. Cell Develop. Biol.* **11**, 441-469.

Xiao, C., Mileva-Seitz, V., Seroude, L. and Robertson, R. M. (2007). Targeting HSP70 to motoneurons protects locomotor activity from hyperthermia in Drosophila. *Dev Neurobiol* **67**, 438-55.

Ye, X., Deng, Y. and Lai, Z. C. (2012). Akt is negatively regulated by Hippo signaling for growth inhibition in Drosophila. *Dev Biol* **369**, 115-23.

Yepiskoposyan, H., Egli, D., Fergestad, T., Selvaraj, A., Treiber, C., Multhaup, G., Georgiev, O. and Schaffner, W. (2006). Transcriptome response to heavy metal stress in Drosophila reveals a new zinc transporter that confers resistance to zinc. *Nucleic Acids Res* **34**, 4866-77.

Zhang, S., Guo, X., Chen, C., Chen, Y., Li, J., Sun, Y., Wu, C., Yang, Y., Jiang, C. and Li, W. (2016). dFoxO promotes wingless signaling in Drosophila. *Scientific reports* **6**, 22348.

Zorzi, E. and Bonvini, P. (2011). Inducible hsp70 in the regulation of cancer cell survival: analysis of chaperone induction, expression and activity. *Cancers (Basel)* **3**, 3921-56.